COLLISION-INDUCED TRANSPORT PROCESSES IN PLANETARY RINGS

GLEN R. STEWART
NASA Ames Research Center

D. N. C. LIN and PETER BODENHEIMER
Lick Observatory

The physics of collision-dominated particle disks around planets is analyzed from both the analytical and numerical point of view. The existence of Saturn's ringlet structure is analyzed in terms of a radial instability induced by viscous diffusion. The detailed model described is based on the assumption of uniform particle size. Modifications caused by finite particle size, gravitational effects, and a distribution of particle sizes are discussed.

I. GENERAL PHYSICAL PROPERTIES OF PLANETARY RINGS

Recently, data obtained from spacecraft and groundbased measurements have greatly refined our knowledge of the rings of Saturn (see chapter by Cuzzi et al.). In particular, the data indicate: (1) a vertical thickness of at most 150 m, and probably several times less (Lane et al. 1982), compared to a radial extent of about 10^{10} cm; (2) the rings are mostly composed of ice particles ranging from cm to m in size (Marouf et al. 1983); and (3) the rings are subdivided into a large number of ringlets with radial dimensions ranging from several hundred km down to the 10-km resolution of the Voyager spacecraft cameras (Smith et al. 1982). Many of these ringlets are observed in the B Ring where they show optical depth variations of 20 to 50% about a mean optical depth ranging from 0.6 to 3.0.

The investigation and explanation of the dynamical features of the rings have fascinated theoreticians over the past several centuries. Critical developments were provided by Maxwell (1859), who deduced that the rings were made up of a large number of orbiting particles, and by Jeffreys (1916, 1947) who was the first to realize that the particles in the rings frequently collide with each other. Jeffreys further showed that dissipation due to these collisions would rapidly flatten the system into a thin disk with a thickness of the order of a few particle diameters, and, on a longer time scale, would tend to spread the ring out in a radial direction. Contemporary researchers have concentrated on more detailed mathematical formulations of the collisional dynamics and the resultant transport processes. Such a description is essential if we are to deduce the basic mechanisms that determine the thickness, cause the radial structure, and regulate the overall evolution of the ring system. For example, we may ask whether the rings have a long enough evolution time scale to have existed for the lifetime of the solar system. A well-established model for the collisional dynamics of ring particles is also required when one considers the tidal interaction between Saturn's inner satellites and the rings. Some features in the rings such as density waves and sharp ring edges have been attributed to these interactions (see chapters by Borderies et al. and by Shu). A third example is the question of the stability of collisional evolution of the rings. Some features such as the density variations in the B Ring may be caused by a diffusion instability.

In this first section we discuss in an approximate way the important physical processes governing the evolution of a collisional particle ring. In later sections we discuss numerical simulations (Sec. II) and in a more rigorous fashion, the equations governing the evolution, first on the basis of kinetic theory (Sec. II) and then on the basis of the fluid approximation (Sec. III). In Sec. III we also analyze the energy budget and energy redistribution in an evolving particle disk. From these analyses, the evolution time scale of the rings as well as their thickness is deduced.

Having constructed a dynamical model for the rings, we examine in Sec. IV the stability of the system. In particular, we establish a general criterion that can be used to determine both the thermal and diffusive stability. This criterion is found to depend critically on the particular form of the coefficient of restitution as a function of impact velocity. We show that rings with optical depth of order unity are unstable and have a tendency to diffuse into ringlets. Qualitative comparisons between theoretical models and the observed radial structures in Saturn's rings are also presented. In Sec. V we discuss how the theory is modified if the finite size of the particles and interparticle gravitational effects are taken into consideration. Finally, in Sec. VI, we make some attempts towards incorporating the effects of a realistic distribution of particle sizes with a simple idealized model. We show that the density variations in large and small particles may be very different in the unstable regions. Section VII summarizes our conclusions.

A. The Role of Collisions

A planetary ring system, like Saturn's, consists mostly of small particles in nearly circular orbits about the central planet. Between successive collisions with other particles, the motion of an individual particle is described by Kepler's laws. For circular orbits the angular frequency of a particle is $\Omega = (GM/r^3)^{\frac{1}{2}}$ where r is the distance from the central mass M. We now estimate the importance of collisions in a disk system of *identical* particles. The collision frequency ω_c can be obtained in terms of the particle density (number per volume) N, the cross section πR_p^2 of a typical particle of radius R_p, and the velocity dispersion c, such that $\omega_c = R_p^2 Nc$. The scale height H of the disk is given by $NH = \sigma/m$, where σ is the surface density in g cm^{-2} and m is the mass of a particle. If the velocity dispersion, which characterizes the random motion of the particles with respect to the local circular orbit, is approximately isotropic, then $H = c/\Omega$ (derived in Sec. II.B.3). Then $\omega_c = R_p^2 \sigma \Omega/m = \tau\Omega/\pi$, where the optical depth $\tau = \pi R_p^2 \sigma/m$ by definition. Thus in regions where $\tau = 1$, as, for example, in portions of Saturn's rings, a typical particle has a collision with a neighboring particle at least twice per orbit. Since orbital periods in planetary-ring systems range from a few hours to a few days, even if τ is as low as 10^{-3}, a particle would still experience a billion collisions during the lifetime of the solar system. Thus collisions are clearly an important process (see chapter by Weidenschilling et al.).

Suppose we start with a set of particles in eccentric and mutually inclined prograde orbits about the central mass M. Collisions between particles tend to dissipate relative kinetic energy and thus to damp relative motion. In a few collision times this process should result in evolution towards coplanar, circular orbits (Jeffreys 1947). As a simple idealized example consider two coplanar particles with identical eccentricities e colliding at a distance r from M, when one particle is at pericenter and the other at apocenter. Because of angular momentum conservation the former is moving faster than the circular velocity at radius r while the latter is moving more slowly. In the case of a purely inelastic collision, the relative motion is completely damped so that the two particles move in the same circular orbit with the same total angular momentum as in the original orbits. Meanwhile, the total energy has decreased by the amount of their original relative kinetic energy, which is given by $\sim e^2\, GM/(2r)$. Similarly, collisions between particles in mutually inclined orbits (inclinations $\pm\, i$) result in damping of relative kinetic energy ($\sim 2i^2\, GM/r$) and establishment of coplanar orbits with the same total angular momentum.

Now consider the situation when the system has approached the disk state with nearly circular and coplanar orbits. The relative motion between particles is now dominated by the radial gradient in the circular orbital velocity. The system will continue to evolve toward a state of lower energy because energy is dissipated during collisions. To illustrate the form that this evolution takes,

we consider two particles in nearly coplanar, circular orbits. The total energy is $\mathscr{E} = m\,(E_1 + E_2)$ and the total angular momentum per unit mass is $J = J_1 + J_2$ where

$$E = J_i^2/2r_i^2 - GM/r_i \tag{1}$$

and

$$J_i = (G\,M\,r_i)^{\frac{1}{2}}\,. \tag{2}$$

The change in the energy of a particle results from changes in both J_i and r_i. However, as already noted above, collisions on the average will tend to circularize orbits. Hence, for the purpose of calculating average energy changes, transitions due to collisions can be thought of as changes from one circular orbit to another. In this case a change in energy can be expressed solely in terms of a change in angular momentum:

$$\frac{\mathrm{d}E}{\mathrm{d}J} = \frac{J}{r^2} = \Omega\,. \tag{3}$$

The change in E caused by a change in r can be ignored because for circular orbits

$$\left.\frac{\partial E}{\partial r}\right|_{J\,=\,\mathrm{const}} = -\frac{J^2}{r^3} + \frac{GM}{r^2} = 0\,. \tag{4}$$

Now consider a small change in the individual angular momenta of the two particles, keeping total angular momentum constant. We have

$$\mathrm{d}\mathscr{E} = m\left(\frac{\mathrm{d}E_1}{\mathrm{d}J_1}\,\mathrm{d}J_1 + \frac{\mathrm{d}E_2}{\mathrm{d}J_2}\,\mathrm{d}J_2\right)$$

$$= m\,\mathrm{d}J_1\,(\Omega_1 - \Omega_2) = m\,\sqrt{GM}\,\mathrm{d}J_1\left(\frac{1}{r_1^{3/2}} - \frac{1}{r_2^{3/2}}\right) \tag{5}$$

since $\mathrm{d}J = \mathrm{d}J_1 + \mathrm{d}J_2 = 0$. Thus for $r_1 > r_2$, $\mathrm{d}\mathscr{E} < 0$ if $\mathrm{d}J_1 > 0$. This argument was used by Lynden-Bell and Pringle (1974) to show that evolution toward a lower energy state is achieved by exchanging angular momentum in the direction such that particles in orbits with smaller semimajor axes give up angular momentum to those in orbits with larger semimajor axes. They use a similar argument to show that energy is also reduced by a net movement of mass to smaller radii.

The overall effect of collisions is thus first to circularize the orbits on a short time scale and then, on a much longer time scale to transport angular

momentum from the inner to the outer region of the disk. The angular momentum transport results in transport of some mass toward the outer edge, but the bulk of the mass must drift inward as a result of the continual dissipation, which must be supplied from the gravitational energy of the disk.

This continual liberation and subsequent dissipation of energy will tend to maintain a small finite velocity dispersion. The minimum possible relative velocity of particles in nearby circular orbits, caused by the difference in angular velocity across one particle diameter $2R_p$, is ΩR_p. Since the orientation of contact of particles at collision will be nearly random, interchange between motions in different directions remains possible. As a result, a finite velocity dispersion in the vertical direction of order ΩR_p is unavoidable (Jeffreys 1947). If the velocity dispersion becomes much larger than ΩR_p, then the mean motion will no longer dominate the outcomes of the collisions and the rapid damping of random motions described at the beginning of this section will dominate. The disk will tend toward a steady state with a thickness on the order of a few particle radii. The efficiency of the angular momentum and mass transfer process in the disk is determined by the collision frequency and the mean free path of particles. Thus the structure and evolution of the system is determined by the detailed properties of the collisions.

B. Transport Processes

From the data mentioned above, we can deduce that each ringlet is composed of a large number of particles. Hence, any theory of the formation of these large-scale structures must ultimately abandon the detailed description of individual particle trajectories and adopt either a statistical mechanical or a fluid-dynamical formulation (see Sec. II.B.1) which describes the average behavior of a collection of particles as a whole. In this section (I.B) we estimate evolutionary time scales for significant radial spreading of the rings using these two approaches. We then (in Sec. I.B.3) consider the fundamental condition for energy balance and the role of the coefficient of restitution in establishing this balance. These concepts will be used in following sections to construct the steady-state vertical structure of the rings and to establish the stability of the steady state.

1. Statistical Properties of Particles in Planetary Rings. The random orientation of deviations from the local circular orbit effectively reduces the most important aspect of the particles' dynamical evolution to a 1-dimensional flow, i.e., a spreading in the radial direction. In a planetary ring with a moderate optical depth, a particle usually travels over a distance comparable to the circumference of an orbit between successive collisions. However, most of this journey is traveled in the tangential direction. Since we are primarily interested in efficiency of diffusion in the radial direction, the typi-

cal radial excursion between successive collisions may be regarded as the relevant scale for the mean free path.

If a typical particle experiences at least two collisions per orbit around the central planet (i.e., $\omega_c \geqslant \Omega/\pi$ or alternatively $\tau \geqslant 1$), this radial mean free path is approximately $\lambda = c/\omega_c$. If the number of particles in a ring is relatively sparse (i.e., $\tau << 1$), the collision frequency may be small compared with the orbital frequency. In this case, the radial excursion of the particle is bounded by its orbital eccentricity e so that the mean free path approaches its upper limit of $ae \simeq c/\Omega$ where a is the semimajor axis of the orbit. For arbitrary τ both limiting values of λ may be included in a single prescription (Cook and Franklin 1964; Goldreich and Tremaine 1978) such that

$$\lambda^2 = c^2 \Omega^{-2} (1 + \tau^2)^{-1} . \tag{6}$$

The above form of the mean free path is entirely analogous to that for a plasma whose motion is confined by a magnetic field (Spitzer 1962). For a typical particle, the mean radial excursion after n such collisions may be approximated by the random-walk expression, $\Delta r = n^{\frac{1}{2}} \lambda$. Thus, the time scale t_{RW} required for a typical particle to randomly walk over a distance Δr is

$$t_{\mathrm{RW}} = \frac{n}{\omega_c} = \frac{1 + \tau^2}{\tau} \Omega \left(\frac{\Delta r}{c} \right)^2 . \tag{7}$$

The above results indicate that a particle can diffuse over a distance > 10 ae on a time scale $100\,(1 + \tau^2)/(\tau\Omega)$ which is longer than both the dynamical (orbital) and collisional time scales. So far, we have ignored the change in τ and c as a result of radial spreading. Thus the above "instantaneous" estimate may be applied to relatively small but not to arbitrarily large radial spreading.

2. *Collective Nature of the Particles*. In a typical planetary ring, the particles' mean free path λ is normally much smaller than the radial extent of the ring. Provided that the disk properties do not vary too rapidly with radius, we may choose a radial scale, Δa, which is both much smaller than L, the scale over which there is appreciable change in the physical properties of the ring, and much larger than λ. Over Δa, the particles have very similar kinematic properties so that their physical properties may be analysed in a collective manner. This aspect of the ring dynamics satisfies the requirements for a fluid description (Boyd and Sanderson 1969). In practice, since the mean free path in the radial direction is limited by the eccentricity of the orbit such that $\lambda \leqslant ae$, a collection of particles contained in a ring of width Δa may be regarded as a basic fluid element provided that $\Delta a > 10\,ae$ and the collisionally induced dynamical evolution is stable on this scale.

The spreading rate may, therefore, also be obtained from fluid dynamics. This approach has been applied to the studies of gaseous accretion disks

(Lynden-Bell and Pringle 1974). In this case, the combined presence of viscosity and differential rotation induces a viscous stress that leads to an outward transfer of angular momentum and a general spread of a ring. The efficiency of angular momentum transfer is determined by the magnitude of the viscosity ν. If ν is a function of position only, the time scale for spreading in the radial direction is $t_\nu \simeq (\Delta r)^2/\nu$ (Lynden-Bell and Pringle 1974), as long as the radial spreading is small enough so there is not a substantial change in ν. The basic expression for the viscosity is $\nu = \omega_c \lambda^2$, so that

$$t_\nu \simeq \frac{1+\tau^2}{\omega_c} \Omega^2 \left(\frac{\Delta r}{c}\right)^2 \tag{8}$$

Since $\tau = \pi\omega_c/\Omega$, t_ν is determined by the identical physical parameters as in the heuristic kinetic argument (see Eq. 7).

3. Energy Transport Processes. Both the kinetic and fluid treatments of diffusion processes indicate that ν is a function of τ and c. Thus, the determination of the magnitude of ν requires a prescription for the velocity dispersion which can be established through consideration of the detailed energy transport processes. Consider two neighboring particles with nearly circular orbits separated by a radial mean free path. The difference between their precollisional circular velocities is of order $\lambda\Omega$. After a collision they will move apart with a comparable velocity difference but their orbits will be reoriented. Consequently, they will each acquire an orbital eccentricity of the order $\lambda/a = c/\Omega a$. The energy change per unit mass associated with this gain in the eccentricity is of the order $(\lambda/a)^2 (\Omega a)^2 = \lambda^2\Omega^2$. Since the kinetic energy per unit mass associated with eccentric motions is, in practice, the energy associated with dispersive random motion, i.e. c^2, its rate of increase may be determined in terms of the collision frequency ω_c such that $\dot{E}_t \simeq c^2\,\omega_c \simeq \lambda^2\Omega^2\,\omega_c$. In the fluid approach, this tendency for increases in c is normally attributed to the effect of viscous stress. In a differentially rotating disk, the viscous stress continually converts energy, from that stored in the systematic shearing motion into that associated with random motion, at a rate

$$\dot{E}_t = \nu\,(r\,\partial\Omega/\partial r)^2 \tag{9}$$

per unit mass, which is of the order $\nu\Omega^2$ for Keplerian orbits. With the substitution of the above formula for viscosity, the hydrodynamic treatment once again provides us with results indentical to those obtained from the kinetic approach.

In the absence of any dissipative process, the collection of particles would be "heated up" in the sense that the dispersion velocity would increase indefinitely. However, typical collisions between particles in the ring are partially inelastic. In the standard terminology for elasticity theory the amount of energy dissipation may be quantified with a coefficient of restitution ϵ

having values between zero (totally inelastic) and unity (perfectly elastic). Formally, ϵ may be expressed in terms of the relative velocities $\mathbf{g}_b \equiv \mathbf{v}_{1b} - \mathbf{v}_{2b}$ and $\mathbf{g}_a \equiv \mathbf{v}_{1a} - \mathbf{v}_{2a}$, before and after a collision between two particles. The central premise of the inelastic hard-sphere model states that the collisional change in relative velocity is proportional to the component of the relative velocity normal to the impact surface such that

$$\mathbf{g}_a - \mathbf{g}_b = -(1+\epsilon)(\mathbf{g}_b \cdot \hat{\mathbf{k}})\hat{\mathbf{k}} \tag{10}$$

where $\hat{\mathbf{k}}$ is the unit vector pointing from the center of particle 1 to the center of particle 2. In planetary rings, the typical value of the impact velocity (which we write as $v_c = |\mathbf{g}_b| = g$) is normally comparable to the dispersion velocity so that an amount $(1-\epsilon^2)\,c^2$ of the kinetic energy per unit mass associated with random motion is dissipated into heat after each collision and is eventually radiated away from the system. The total number of collisions per unit time interval in the disk is ω_c so that the total rate of energy dissipation per unit mass is

$$\dot{E}_d = (1-\epsilon^2)\,c^2\omega_c\ . \tag{11}$$

At any radial position in the rings, the local kinetic energy associated with random motion may be changed by several other energy transport processes such as the advective transport caused by the bulk motion of the particles and the conductive transport induced by collisions between particles. However, these processes are normally much less efficient than the above local energy-generation and energy-dissipation mechanisms. Thus, a local energy equilibrium can only be established if these two processes are delicately balanced. The condition for energy balance is

$$\dot{E}_d = \dot{E}_t\ . \tag{12}$$

The above equation implies the following relationship between ϵ and τ for a disk with uniform particle size:

$$(1-\epsilon^2)(1+\tau^2) = b \tag{13}$$

where b is a constant of order unity (Cook and Franklin 1964; Goldreich and Tremaine 1978). This equilibrium $\epsilon-\tau$ relation does not explicitly depend on the velocity dispersion because both $\dot{E}_t$ and $\dot{E}_d$ have the same velocity dependence. In general $\dot{E}_t$ would have a different velocity dependence than $\dot{E}_d$ (if, e.g., we had included gravitational interactions between particles) and the energy balance would determine an explicit formula for the equilibrium velocity dispersion (Safronov 1969; see also chapter by Ward). In the present case, the equilibrium velocity may be determined from Eq. (13) once the depen-

dence of ϵ on impact velocity is specified. Equation (13) also establishes a relation between ν and c, since $\nu = \omega_c \lambda^2$ and λ is given by Eq. (6).

If ϵ is independent of v_c, the rings may never establish an energy equilibrium and would either expand into a torus or collapse into a monolayer disk. This evolutionary tendency, which occurs because an increase in the velocity dispersion due to collisions is not compensated by an increase in dissipation, is somewhat analogous to thermal instabilities in accretion disks (Pringle et al. 1973; Shakura and Sunyaev 1976; Faulkner et al. 1983). However, ϵ for various rocky and metallic materials has been measured experimentally and found to be a monotonically decreasing function of v_c (Goldsmith 1960; see Sec. IV.B.1 for further discussion). If the ring particles have similar mechanical properties, the low-velocity collisions are much more elastic than high-velocity impacts. Consequently, for a ring with a particular τ, $\dot{E}_d$ increases faster than c^2 while $\dot{E}_t$ increases only as fast as c^2. Thus, for small c, the collisions would be mostly elastic so that $\dot{E}_t > \dot{E}_d$. In this case, the velocity dispersion of the particles would increase exponentially until ϵ were reduced to a small enough value such that $\dot{E}_t = \dot{E}_d$. Alternatively, for large c, $\dot{E}_d$ could be greater than $\dot{E}_t$ so that the kinetic energy stored in random motion would be continually drained until c were sufficiently small to establish an energy equilibrium. In the case that gravitational scattering is a significant energy source for random motion, a stable energy equilibrium can be established even if ϵ is independent of velocity because the effectiveness of gravitational scattering decreases with increasing relative velocity (chapter by Ward; also see Sec. V.A.1 below).

The above heuristic arguments indicate that, if ϵ is a decreasing function of v_c, not only is there an energy equilibrium, but this equilibrium is stable. In a particle ring, the energy equilibrium is established on the time scale for energy to diffuse through the thickness of the ring. For a semitransparent ring, this time scale is comparable to the orbital period (Goldreich and Tremaine 1978). Since the ringlet structure in Saturn's rings appears to be persistent over times much longer than the orbital period, it is reasonable to assume that these regions are in an energy equilibrium. Then, as shown above, the energy balance equation constrains $\epsilon(\tau)$. If $\epsilon(v_c)$ were known, this constraint would lead to $c(\tau)$ and $\nu(\tau)$ relationships which could be used to examine the evolution of the rings through solutions of the momentum equation alone.

II. MATHEMATICAL FORMULATION: KINETIC THEORY

A. Numerical Simulation

The collective physical processes, which were heuristically described above, occur on the length scale of a few mean free paths and on a time scale comparable to the orbital period. These length and time scales are much too small to be resolved by any current observations so that it is rather difficult to

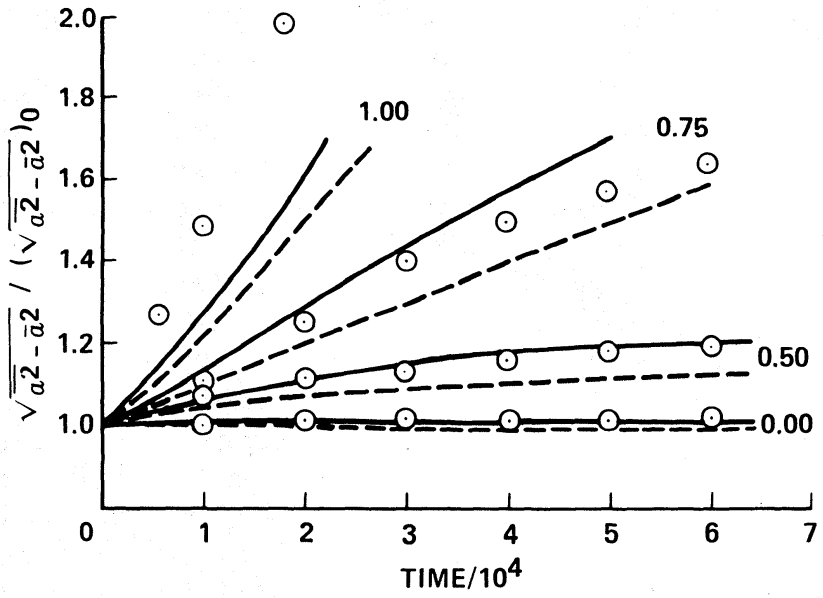

Fig. 1. The evolution of the distribution of particles' semimajor axes $(\overline{a^2}-\bar{a}^2)^{\frac{1}{2}}$. The subscript zero refers to the initial state. Curves are labeled with value of ϵ. *Open circles:* numerical calculation by Hämeen-Anttila and Lukkari (1980). *Solid curves* and *dashed curves:* results of two different analytical calculations by Hämeen-Anttila (1978). Times are given in units of the orbital period (figure from Hämeen-Anttila and Lukkari 1980).

directly compare theories with observations. However, the results of numerical simulation may be compared with theoretical arguments to verify the validity of various assumptions and to identify the key processes which dominate the evolution of the system. In the simulations of Trulsen (1972*a*), Brahic (1977), and Hämeen-Anttila and Lukkari (1980), the particles are modeled as identical rigid spheres which interact according to the hard-sphere collision model often used to simulate molecular dynamics. To simulate particle rings a degree of dissipation in the collisions must be included according to Eq. (10). The advantage of this idealized prescription is that comparisons between numerical and analytic solutions may be readily obtained.

The first step in a numerical simulation is to examine the simplest evolutionary tendencies, e. g., the radial spreading of a particle disk due to collisions. This effect is measured by the secular changes in the distribution of the particles' semimajor axes $(\overline{a^2}-\bar{a}^2)^{\frac{1}{2}}$ (Hämeen-Anttila and Lukkari 1980). According to the arguments in Sec. I, the rate of change in $(\overline{a^2}-\bar{a}^2)^{\frac{1}{2}}$ must be a function of ϵ. This qualitative expectation is indeed confirmed by the results of the numerical simulation. In Fig. 1, the circles denote simulations for several (constant) values of ϵ whereas the solid and dashed lines outline the results of two different analytic calculations by Hämeen-Anttila (1978). There is a general agreement between the numerical and analytic results.

As the evolution proceeds, the ring's thickness is automatically adjusted to establish an equilibrium velocity dispersion and scale height. The simula-

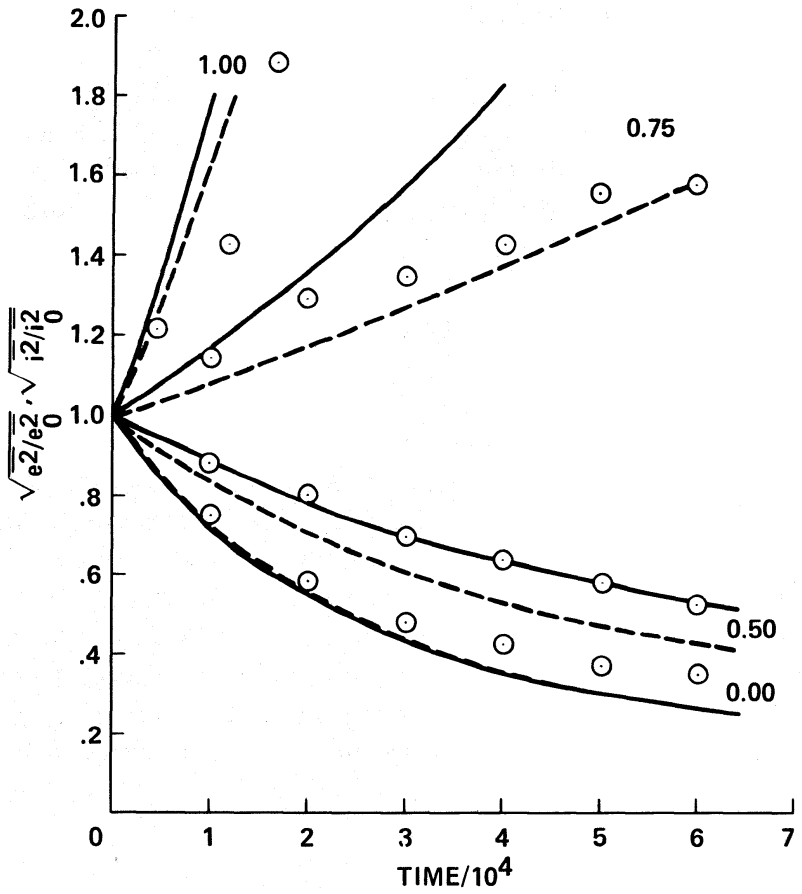

Fig. 2. The evolution of the mean eccentricity $(\overline{e^2})^{\frac{1}{2}}$ and the mean inclination $(\overline{i^2})^{\frac{1}{2}}$. Both sets of curves have been normalized to unity at $t = 0$ and are the same within the resolution of the plot. Notation is the same as in Fig. 1 (figure from Hämeen-Anttila and Lukkari 1980).

tions illustrate the rapid initial flattening and radial spreading of the system. The outcome is critically dependent on the prescription for ϵ that determines the rate of dissipation of orbital kinetic energy. Hämeen-Anttila and Lukkari's (1980) numerical simulations show how the ring settles into a flat-disk structure with root-mean-square orbital eccentricities and inclinations comparable to R_p/a if collisions are very inelastic (Fig. 2). Conversely, for highly elastic collisions, the ring evolves into a thick torus (Fig. 2). For moderate values of ϵ (e.g., $0.5 < \epsilon < 0.75$), the velocity dispersion may be maintained at an approximately constant value. Their analytic results also show similar evolutionary tendencies. Numerical simulations in which ϵ decreases with velocity of impact have also been carried out. Incorporating the prescription $\epsilon = \exp(-kv_c)$, where k is a constant, Hämeen-Anttila and Lukkari found that the velocity dispersion adjusted to allow energy equilibrium.

Regardless of the detailed prescription for ϵ, the orbital eccentricity and inclination quickly establish a quasi stationary equilibrium distribution of the form

$$F(x) = x^n \exp(-Cx^2/\bar{x^2}); x = e, i \tag{14}$$

with the power index n slightly less than unity (Trulsen 1972*a*). One possible interpretation for this dynamical property is that there is a general tendency for F to relax quickly into a maximum entropy state allowed under various collisional constraints. In such a state the particles assume a Gaussian distribution of random kinetic energy such that

$$F(E) \sim \exp(-Cx^2/\bar{x^2}); x = e, i. \tag{15}$$

The corresponding distribution for e and i is a Rayleigh distribution which has a functional form similar to Eq. (14) with $n = 1$. Since there are two degrees of freedom associated with the planar motion, the energy equipartition induces $(\bar{i^2}/\bar{e^2})^{\frac{1}{2}} = 1/\sqrt{2}$, if collisions are isotropic. Numerical simulations do in fact evolve to states near energy equipartition in e and i (see e.g., Trulsen 1972*a*). If ϵ is very small, particles settle down in a near-monolayer structure such that the orientation of colliding bodies (specified by $\hat{\mathbf{k}}$) becomes anisotropic with a preferred orientation in the plane of the rings. Hence, the random motion associated with orbital eccentricities is damped more efficiently than the motion due to orbital inclinations. Both numerical simulations and analytic solutions indicate that the ratio $(\bar{i^2}/\bar{e^2})^{\frac{1}{2}}$ decreases with increasing ϵ (Fig. 3).

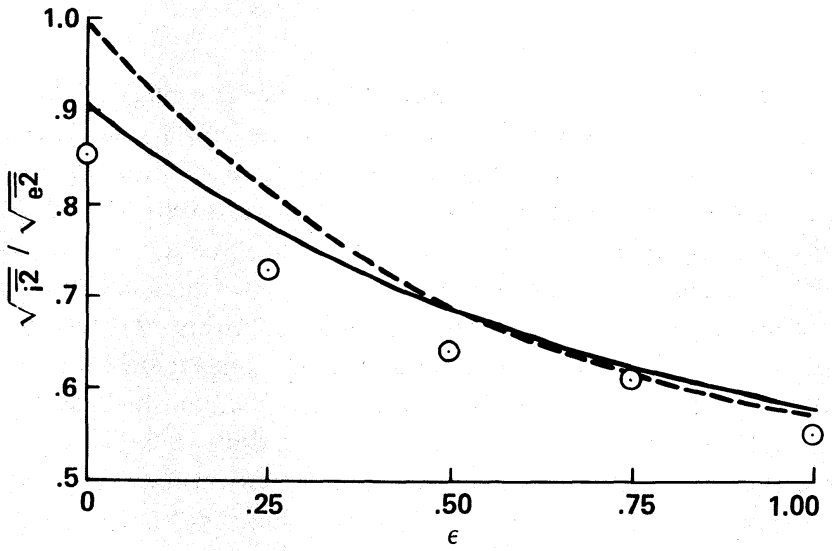

Fig. 3. The stationary value of $(\bar{i^2}/\bar{e^2})^{\frac{1}{2}}$ as a function of ϵ. Theoretical calculations (solid and dashed curves) and numerical simulations (open circles), as well as the figure itself, come from the work of Hämeen-Anttila and Lukkari (1980).

In contrast to the above studies of hard-sphere collisions, Trulsen (1972*b*) considered a more general collision model, the so-called snowflake model. Because of the assumed fluffy structure of the particles, this collision model led to an enhanced energy dissipation for grazing collisions, i.e., those which are most effective at producing random motions. When this model was used in a 2-dimensional simulation (all particles in the same plane) a small degree of radial focusing and clustering of pericenter arguments was observed. Brahic and Hénon (1977) made a preliminary test of a similar collision model in 3 spatial dimensions but did not report any results concerning radial clumping. Another mechanism, which can produce very definite local density enhancements, is the so-called diffusion instability, discussed in Sec. IV, which can occur even in the hard-sphere collision case as long as the coefficient of restitution is a decreasing function of impact velocity.

B. Analytical Approach.

The qualitative reasoning provided in Sec. I is too general to provide a deep appreciation of the detailed evolutionary characteristics. Due to the limitation of computers, numerical simulations are normally carried out with relatively coarse spatial resolution, limited number of particles, and for relatively short time scales. In order to make further progress towards a general understanding of the dynamics of planetary rings, rigorous mathematical analyses are necessary. In this section we discuss the dynamics from the point of view of the kinetic theory of gases.

1. Boltzmann Equation. The statistical properties of the particles may be expressed in terms of a probability density $f(m, r, \mathrm{v}, t)$ for finding a particle of mass m at position r with velocity v at time t. Alternatively, f may be referred to as the distribution of particles in position-momentum space. In terms of f, the evolution of the system is described by the Boltzmann equation

$$\left(\frac{\partial}{\partial t} + \mathrm{v}_i \frac{\partial}{\partial x_i} - \frac{\partial U}{\partial x_i} \frac{\partial}{\partial \mathrm{v}_i}\right) f(m) = \sum_j \mathscr{C}[f(m), f(m_j)] \qquad (16)$$

where x and v are the position and velocity, respectively, expressed in some orthonormal coordinates. $U(x)$ is the gravitational potential due to the planet, its satellite system, any massive satellites that are imbedded in the rings and not included in the collection of particles described by f, and the self gravity of the particles included in the distribution function f. The right-hand side of the above equation represents the rate of change of f caused by collisions with particles of mass m_j.

The complexity of the collision integral generally prevents an exact solution of the Boltzmann equation. Considerable simplification can be achieved

by replacing it with three sets of moment equations, obtained through multiplication, respectively, by 1, v_i, and $v_i v_j$, and integration over all velocities (e.g., Goldreich and Tremaine 1978):

$$\frac{\partial N}{\partial t} + \frac{\partial}{\partial x_i}(Nu_i) = \left(\frac{\partial N}{\partial t}\right)_c \tag{17}$$

$$\frac{\partial}{\partial t}(Nu_i) + \frac{\partial}{\partial x_j}(p_{ij} + Nu_i u_j) + \frac{N\partial U}{\partial x_i} = \left[\frac{\partial}{\partial t}(Nu_i)\right]_c \tag{18}$$

$$\frac{\partial}{\partial t}(p_{ij} + Nu_i u_j) + \frac{\partial}{\partial x_k}(p_{ijk} + u_j p_{ik} + u_k p_{ij} + u_j p_{jk}$$

$$+ Nu_i u_j u_k) + N\left(u_i \frac{\partial U}{\partial x_j} + u_j \frac{\partial U}{\partial x_i}\right) = \left[\frac{\partial}{\partial t}(p_{ij} + Nu_i u_j)\right]_c \tag{19}$$

where

$$N = \int f d^3v, \; Nu_i = \int f v_i d^3v$$

$$p_{ij} = \int f (v_i - u_i)(v_j - u_j) d^3v \; . \tag{20}$$

In general, u_i consists of the local Keplerian circular velocity plus the radial flow generated by viscous evolution. These equations are entirely analogous to the moment equations of the kinetic theory of gases. This procedure of replacing the particle distribution function in the Boltzmann equation with its first three velocity moments is commonly referred to as the "hydrodynamic approximation." Note that this level of approximation is more general than the true "fluid" description given in Sec. III, which makes the further approximation that the diagonal components of pressure tensor p_{ij} are equal and thus may be replaced by a scalar pressure p.

In this treatment the physical processes which essentially determine the evolution of the rings are contained in the collision terms. For example, the term $(\partial N/\partial t)_c$ describes the evolution of the distribution function f due to coagulation and shattering whereas the term $[\partial(Nu_i)\partial t]_c$ includes, in addition, the effects of particle spin. The term $(\partial p_{ij}/\partial t)_c$ is due to contributions from gravitational scattering and inelastic collisions among the disk particles themselves. If all of these contributions are included at once, the mathematical complexity of the solution may easily obscure a general appreciation of the basic dynamical characteristics of the rings. Thus, it is advantageous to analyse the problem piecewise by considering only the dominant processes first. The simplest approach is to assume that the planetary rings are made of identical, hard, indestructible, nonspinning spheres, so that

the collisional contribution to the zeroth- and first-moment equations (i.e., the right-hand sides of Eqs. (17) and (18) may be ignored). However, the effects of collisions in the second moment equation may not be ignored because these effects are essential for determining an energy equilibrium.

With the above assumption, the zeroth-moment equation is reduced to a simple continuity equation in which the evolution of the particle distribution function is determined by the gradient of the particle flux. The evolution of the flux may be readily obtained from the simplified first-order moment equation; it is determined by the gradient of the planet's gravitational potential and a collective stress due to the gradient in the pressure tensor **p**. Although the gravitational influence of the planet does not change significantly in time, the stress does.

The evolution of the stress tensor must be obtained from the second-order moment equation, which includes both the collisional effects and a contribution from a third-order pressure tensor p_{ijk}. The third order tensor must in turn be determined from a higher order moment equation. Since this mathematical procedure may be continued to arbitrarily high order, the hierarchy of velocity moments must be truncated at some stage. In the standard treatment of the problem (i.e., the hydrodynamic approximation used by Goldreich and Tremaine [1978]), the moment equations are closed by neglecting the third-order velocity moment of f occurring in the second-moment Eq. (19). Provided that the physical parameters such as the number density do not change significantly over a radial scale comparable to the vertical scale height, such an approximation is justified since the third-order velocity moment is smaller than the magnitude of all other contributions in the second-moment equation, by a factor approximately equal to the orbital eccentricity. Through such an approximation the velocity dependence of the probability density is totally constrained once a prescription for the collisional integral is specified.

2. *Collisional Integrals.* In general, the derivation for the collisional integral is rather complex since it contains contributions from various physical processes. Here, standard approximations used to evaluate collisional effects, such as the Fokker-Planck approximations, are not generally applicable because they are usually calculated for small-angle scattering whereas direct collisions in planetary rings result in large-angle scattering. One possible method adopted by Cook and Franklin (1964) is to use a Krook model for collision terms such that $(\partial f/\partial t)_c = \omega_c (f_o - f)$ where f_o is a Maxwellian which has the same number and energy density as f. The disadvantage of this method is that the energy loss due to inelastic collisions is not directly included in the above equations. In order to achieve an energy equilibrium, Cook and Franklin introduce an *ad hoc* prescription to account for the energy loss without altering the basic collision formula; thus the results of their calculations may be an artifact of their adopted assumptions. However, the evaluation of the collisional integral may be simplified considerably with the

adoption of the following assumptions: (1) all particles are identical; (2) all collisions are hard-sphere collisions; (3) the particles' size is small compared with the interparticle spacing; (4) the epicyclic nature of the deviations from coplanar circular orbits is neglected so that the random velocities may be assumed to have a Gaussian distribution. The implications of this last approximation have not been thoroughly investigated, although Baxter and Thompson (1973) and Hämeen-Anttila (1978) have begun work in this direction. Under these assumptions, Trulsen (1971) derived the collisional integral associated with collision law (Eq. 10):

$$\mathcal{C}[f,f] \equiv \left(\frac{\partial f}{\partial t}\right)_c = 4R_p^2 \iint_{(\mathbf{g}\cdot\hat{\mathbf{k}})>0} [f(\mathbf{v}_1^*)f(\mathbf{v}_2^*)/\epsilon^2 - f(\mathbf{v}_1)f(\mathbf{v}_2)](\mathbf{g}\cdot\hat{\mathbf{k}})\mathrm{d}\hat{\mathbf{k}}d^3\mathrm{v}_2 \tag{21}$$

where

$$\mathbf{v}_{1,2}^* = \mathbf{v}_{1,2} \mp \frac{(1+\epsilon)}{2\epsilon}(\mathbf{g}\cdot\hat{\mathbf{k}})\hat{\mathbf{k}} \tag{22}$$

and R_p is the radius of a particle. Substituting this expression into the second-moment equation to replace the collisionally induced pressure tensor term, we find

$$\left(\frac{\partial p_{ij}}{\partial t}\right)_c = \frac{\pi}{12}R_p^2 \int\int (1+\epsilon)\,[(1+\epsilon)g^2\,\delta_{ij} - 3\,(3-\epsilon)\,g_i\,g_j] \times g f(\mathbf{v}_1)f(\mathbf{v}_2)d^3\mathrm{v}_1 d^3\mathrm{v}_2 \tag{23}$$

where δ_{ij} is the identity tensor. A similar expression for the above equation has been obtained by Goldreich and Tremaine (1978) for the special $i = j$ case. In the following discussion we shall use a cylindrical coordinate system (r, θ, z).

In order to evaluate the collision integral in Eq. (23) we must specify the velocity dependence of the distribution function $f(\mathrm{v})$ as well as of the coefficient of restitution ϵ. The results of the numerical simulations indicate that particle energies quickly establish an approximately Gaussian distribution (see Eq. 15). For most analytic treatments of the problem, it is usually assumed (Goldreich and Tremaine 1978; Hämeen-Anttila 1978) that f has a 3-dimensional Gaussian distribution and that it may be expressed in terms of a velocity dispersion tensor $T_{ij} = p_{ij}/N$ such that

$$f = N\,[(2\pi)^3 \det \mathbf{T}]^{-\frac{1}{2}} \exp\,[-\tfrac{1}{2}\mathrm{v}_i(T^{-1})_{ij}\,\mathrm{v}_j]\,. \tag{24}$$

The trace of $\mathbf{T}$ (i.e., $\mathrm{Tr}\mathbf{T} = \mathbf{T}_{11} + \mathbf{T}_{22} + \mathbf{T}_{33}$) equals the mean square of the velocity dispersion, $\overline{c^2}$, due to orbital eccentricity and inclination. The basic motivations for adopting this particular expression are: (1) it satisfies the steady-state solution of the second-moment equation in the limit where collisions have a negligible effect on the evolution of the rings (i.e., $T_{rr} = 4T_{\theta\theta}$; $T_{r\theta} = 0$); (2) it reduces to a Maxwellian form in the isotropic collision dominated limit ($T_{ij} = \mathrm{Tr}\mathbf{T}\,\delta_{ij}/3$); and (3) it attains a nonvanishing $P_{r\theta}$ which induces angular momentum transport and matter redistribution. With minor alterations, a more general distribution function may be constructed to include the asymmetric distributions of pericenter arguments and ascending nodes (Hämeen-Anttila 1978).

Further progress can only be made with additional approximations. The standard procedure to follow at this point is to assume that ϵ has a weak dependence on v_c. Since the relative velocity has a Gaussian distribution, most of the collisions occur with $\overline{c^2} = \mathrm{Tr}\mathbf{T}$. Thus, it may be resonable to treat ϵ as a constant term in the integration and remove terms containing ϵ outside of the integral. The error introduced by this procedure may be simply treated as a deformation of ϵ since it is uncertain anyway (Hämeen-Anttila 1981).

Despite the above approximation, the anisotropy of the tensor $\mathbf{T}$ still prevents the exact evaluation of the integral in Eq. (23). However, it is possible to transform the integration variable into a diagonalized form so that the dimensionality of the integral may be reduced to one. The remaining integral can be evaluated easily over two of the principal axes. After some coordinate transformations, the integral over the third principal axis may also be evaluated if the velocity dependence in ϵ is ignored. The resultant integral can be expressed as

$$\left(\frac{\partial p_{ii}}{\partial t}\right)_c = 4\pi^{\frac{1}{2}} N^2 R_p^{\,2} \frac{(1+\epsilon)}{(p_{jj}p_{kk})^{\frac{1}{2}}} P_{ii}^{\frac{5}{2}} \left[(1+\epsilon)J_p^i + J_q^i\right] \tag{25}$$

where J_p^i and J_q^i are symmetric functions of p_{ii}/p_{jj} and p_{ii}/p_{kk}, respectively, and can be expressed in terms of elliptical integrals (Goldreich and Tremaine 1978). However, the resultant integrals are sufficiently complex so that it is usually more convenient to evaluate them numerically.

Alternatively, the integral may be evaluated analytically under the assumption that one factor of g in the integrand may be approximated by a constant value

$$g_0 = \frac{16}{3}\left(\frac{\mathrm{Tr}\mathbf{T}}{3\pi}\right)^{\frac{1}{2}} \tag{26}$$

(Hämeen-Anttila 1978, 1981). This approximation is analogous to the earlier approximation where terms containing ϵ are pulled out of the integral. The

basis of the approximation is again the Gaussian form of the velocity distribution which implies that the dominant contribution of the integral may be attributed to a sufficiently narrow range of the integration variable that g may be treated as a constant. The numerical coefficient in g_0 was chosen to yield the exact result for the special case of an isotropic velocity distribution. The accuracy of this approximation is tested by a direct comparison with the numerical calculations below. With this approximation, the integral becomes

$$\left(\frac{\partial p_{ij}}{\partial t}\right)_c = \frac{8}{9} N R_p^2 (\pi \mathrm{Tr}\mathbf{T}/3)^{\frac{1}{2}} (1+\epsilon) \left[(1+\epsilon)\,\mathrm{Tr}\mathbf{p}\,\delta_{ij} - 3(3-\epsilon)p_{ij}\right] \quad . (27)$$

3. Mass and Momentum Transfer. With the evaluation of the collisional integral, we now discuss the evolution of the mass distribution in the rings. In order to simplify this analysis, we examine the z-dependence of N with a thin-disk approximation. The basis of this approximation is to assume that the variation of gravitational potential in the vertical (z) direction is relatively small so that the dependence of physical parameters on the two independent spatial variables r and z, may be separated and the general physical properties of the disk may be averaged over the z direction. With this approximation, the dynamics of a disk or a ring may be characterized primarily by the evolution of the surface density $\sigma = m \int N(z)\mathrm{d}z$. To determine $\sigma(r)$ we consider a thin, smoothly varying disk where the thickness $H << r$ and the radial gradient of H, $\mathrm{d}H/\mathrm{d}r$, $<<1$. Then the bulk motion in the vertical direction $u_z \approx (\partial H/\partial r)u_r$ is generally much less than u_r. With the neglect of contributions from u_z the z component of the first-moment equation is reduced to

$$\frac{1}{N}\frac{\partial}{\partial z}\left(NT_{zz}\right) = -\frac{GMz}{r^3} . \quad (28)$$

If we assume T_{zz} is independent of z for a thin ring, we deduce from the above equation that the number density of the disk particles decreases exponentially with z such that

$$N(z) = N(0)\ \exp[-\Omega^2 z^2/(2T_{zz})] \quad (29)$$

where $N(0)$ is the number density at the mid-plane. Consequently, the vertical scale height $H \cong (T_{zz})^{\frac{1}{2}}/\Omega$. Integrating $N(z)$ over z we find $\sigma = N(0)$ $m(2\pi T_{zz})^{\frac{1}{2}}/\Omega$ which also implies $\tau = \pi R_p^2 \sigma/m \approx \omega_c/\Omega$.

If T_{ij} is independent of z, $\int p_{ij}\,\mathrm{d}z = \sigma/m\ T_{ij}$ and the first-order moment equation reduces to

$$\frac{\partial u_r}{\partial t} + u_r\frac{\partial u_r}{\partial r} - \Omega^2 r = -\frac{GM}{r^2} + T_{\theta\theta} - \frac{1}{\sigma r}\frac{\partial}{\partial r}(r\sigma T_{\theta\theta}) \quad (30)$$

and

$$\frac{\partial}{\partial t}(\Omega r) + \frac{u_r}{r}\frac{\partial}{\partial r}(r^2\Omega) = -\frac{1}{\sigma r^2}\frac{\partial}{\partial r}(r^2\sigma T_{r\theta}) \ . \qquad (31)$$

The dominant terms in Eq. (30) are $\Omega^2 r$ and GM/r^2 unless either σ or $T_{\theta\theta}$ varies significantly over a characteristic length scale L comparable to H. For a typical, thin, smoothly varying disk, L is generally much larger than H so that Eq. (30) merely provides a requirement for the rotation law to be Keplerian, i.e. $\Omega = (GM/r^3)^{\frac{1}{2}}$ at all times. In this case, equation (31) reduces to

$$\sigma u_r r = \dot{m}/2\pi = \frac{2}{\Omega r}\frac{\partial}{\partial r}(r^2\sigma T_{r\theta}) \ . \qquad (32)$$

The variable $\dot{m}$ may be interpreted as the mass transfer rate in the radial direction. Under the special condition of steady-state flow, i.e., when $\partial\sigma/\partial t = 0$, $\dot{m}$ is independent of radius and

$$u_r \simeq T_{r\theta}/(\Omega r) = T_{r\theta}{}^{\frac{1}{2}}\left(\frac{T_{r\theta}}{T_{zz}}\right)^{\frac{1}{2}}\frac{H}{r} << T_{r\theta}{}^{\frac{1}{2}} << \Omega r \ . \qquad (33)$$

In general, the evolution of the particle distribution in the disk may be obtained from the zeroth-order moment equation:

$$\frac{\partial\sigma}{\partial t} = -\frac{1}{r}\frac{\partial}{\partial r}(r\sigma u_r) = \frac{2}{r}\frac{\partial}{\partial r}\left[\frac{1}{\Omega}\frac{\partial}{\partial r}\left(r^2\sigma T_{r\theta}\right)\right] \ . \qquad (34)$$

4. Evolution of the Pressure Tensor. For the solution of Eq. (34) a $(\sigma, T_{r\theta})$ relationship must be specified; it can be obtained from the second-order moment equation. If we ignore $(\partial N/\partial t)_c$ and $(\partial N u_i/\partial t)_c$ we can write this equation in the simplified form

$$\frac{\partial p_{ij}}{\partial t} + p_{ik}\frac{\partial u_j}{\partial x_k} + p_{jk}\frac{\partial u_i}{\partial x_k} + \frac{\partial}{\partial x_k}\left(p_{ij}u_k\right) + \frac{\partial}{\partial x_k}\left(p_{ijk}\right) = \left(\frac{\partial p_{ij}}{\partial t}\right)_c \qquad (35)$$

In a thin, axisymmetric disk, $p_{rz} = p_{z\theta} = 0$ so that there are only four nonvanishing components of the pressure tensor. However, even if we neglect contributions associated with u_z, vertically average the equations, and assume $L >> H$ (see Sec. II.B.1), the analytic solutions of partial differential Eq. (35) are still not readily transparent without further simplification. In principle the

solution depends on the initial conditions in the ring. However, the results discussed above indicate that the ring tends to evolve into an energy equilibrium state on a relatively rapid time scale. In Sec. IV we shall rigorously demonstrate that such an energy equilibrium state is stable; for the moment we may assume that the pressure tensor is independent of time. Consequently, we may obtain an energy transport equation by summing up all the diagonal elements of T_{ij}:

$$-3\Omega\sigma T_{r\theta} = \left(\frac{\partial}{\partial t}\sigma \,\mathrm{Tr}\mathbf{T}\right)_c \quad . \tag{36}$$

The above equation implies that there is an overall balance between the rate of energy generation by viscous stress and energy dissipation by inelastic collisions. It is of interest to note that when collisions are totally elastic, so that the right-hand side of Eq. (36) is zero, the energy generation term nevertheless appears finite despite the absence of dissipation. However, in this case, steady-state solutions are not permitted so that Eq. (36) is not really applicable.

Equation (36) may be solved numerically with the aid of the numerically integrated values for the collisional integrals (Goldreich and Tremaine 1978). Using this approach, we can establish a relationship between ϵ and τ from the numerical solutions (see Fig. 4), which may be expressed as

$$\epsilon = [1 - b/(1 + \tau^2)]^{\frac{1}{2}} \tag{37}$$

where b is a numerical constant equal to 0.61. This relationship is identical, within a constant factor of order unity, to that derived from the heuristic arguments in Sec. I.

Alternatively, we may utilize the simplified, analytical, approximate solutions for the collisional integrals (Eq. 27). In a thin disk, the second-order moment equation integrated over z becomes:

$$\left(\frac{\partial p_{rr}}{\partial t}\right)_c = \frac{\partial p_{rr}}{\partial t} - 4\Omega p_{r\theta} = \frac{\omega_0}{18}(1+\epsilon)\left[(1+\epsilon)\mathrm{Tr}\mathbf{p} - 3(3-\epsilon)p_{rr}\right] \tag{38a}$$

$$\left(\frac{\partial p_{r\theta}}{\partial t}\right)_c = \frac{\partial p_{r\theta}}{\partial t} - \Omega(p_{rr}/2 + 2p_{\theta\theta}) = -\frac{\omega_0}{6}(1+\epsilon)(3-\epsilon)p_{r\theta} \tag{38b}$$

$$\left(\frac{\partial p_{\theta\theta}}{\partial t}\right)_c = \frac{\partial p_{\theta\theta}}{\partial t} + \Omega p_{r\theta} = \frac{\omega_0}{18}(1+\epsilon)\left[(1+\epsilon)\,\mathrm{Tr}\mathbf{p} - 3(3-\epsilon)p_{\theta\theta}\right] \tag{38c}$$

$$\left(\frac{\partial p_{zz}}{\partial t}\right)_c = \frac{\partial p_{zz}}{\partial t} = \frac{\omega_0}{18}(1+\epsilon)\left[(1+\epsilon)\,\mathrm{Tr}\mathbf{p} - 3(3-\epsilon)p_{zz}\right] \tag{38d}$$

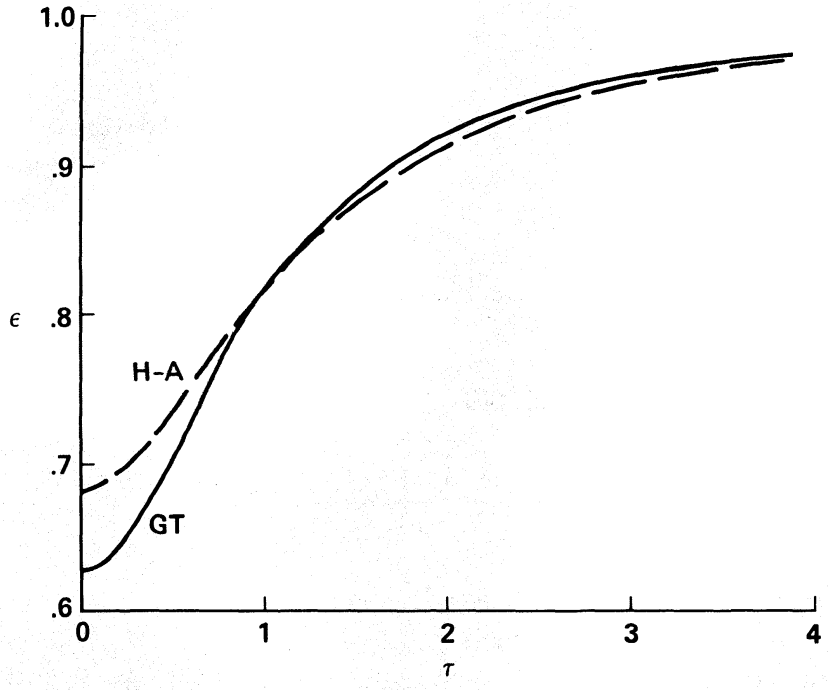

Fig. 4. Comparison between the $\epsilon-\tau$ relations calculated by Hämeen-Anttila (1978), marked H–A, and by Goldreich and Tremaine (1978), marked GT.

where the effective collisional frequency ω_0 can be defined in terms of the optical depth τ such that

$$\omega_0 = \frac{8\tau\Omega}{\pi} (\mathrm{Tr}\mathbf{T}/3T_{zz})^{\frac{1}{2}} . \tag{39}$$

In a steady state, the energy transport Eq. (36) becomes

$$9\Omega T_{r\theta} = \omega_0(1 - \epsilon^2)\ \mathrm{Tr}\mathbf{T}. \tag{40}$$

Substituting this expression for ω_0 back into Eq. (38) we find

$$\begin{aligned} T_{rr} &= \frac{9-7\epsilon}{3(3-\epsilon)}\ \mathrm{Tr}\mathbf{T} \\ T_{zz} &= \frac{1+\epsilon}{3(3-\epsilon)}\ \mathrm{Tr}\mathbf{T} \\ \mathrm{T}_{\theta\theta} &= \frac{3\epsilon-1}{3(3-\epsilon)}\ \mathrm{Tr}\mathbf{T} \end{aligned} \tag{41}$$

so that

$$\frac{\omega_0}{\Omega} = \frac{8\tau}{\pi}\left(\frac{3-\epsilon}{1+\epsilon}\right)^{\frac{1}{2}} = \left[\frac{9(19\epsilon-13)}{(1-\epsilon)}\right]^{\frac{1}{2}} / [(1+\epsilon)(3-\epsilon)] \tag{42}$$

and

$$\tau = \frac{3\pi}{8}\left[\frac{19\epsilon-13}{(1-\epsilon^2)(3-\epsilon)^3}\right]^{\frac{1}{2}}. \tag{43}$$

Inserting this result back into Eq. (40) gives

$$T_{r\theta} = \frac{[(19\epsilon-13)(1-\epsilon)]^{\frac{1}{2}}}{3(3-\epsilon)}\ \mathrm{Tr}\mathbf{T} \tag{44}$$

and, indirectly, a relationship between $T_{r\theta}$ and τ.

The approximate analytic result for the $\epsilon-\tau$ relation in Eq. (43) closely agrees with the numerical result represented by Eq. (37) (see Fig. 4) and thereby provides an a posteriori justification for the approximation adopted by Hämeen-Anttila. The largest deviation between the two solutions occurs for small optical depth because the departure from isotropy in the velocity distribution is greatest at low collision frequencies. With some modifications and a more complex approximation for the collisional integral, a closer agreement between analytic and numerical results may be obtained (Hämeen-Anttila 1978).

5. Collision-induced Viscous Evolution of the Disk. In the previous section, we outlined two methods, both involving a rather restrictive set of assumptions, of obtaining relationships between τ and ϵ and between T_{ij} and $\mathrm{Tr}\mathbf{T}$. These relationships may be used to study the long-term viscous evolution of the disk. Provided that the disk is thermally stable, the thermal equilibrium solutions are fully applicable for this purpose since the time scale for establishing an energy equilibrium is much shorter than the diffusion time scale. The evolution is determined by the solution of the mass diffusion Eq. (34) which contains variables such as σ and $T_{r\theta}$. Thus, in addition to the above results a relationship between τ (or ϵ) and any component of the pressure tensor must be specified before the diffusion equation may be solved as an initial value problem.

If there is a one-to-one correspondence between ϵ and v_c (or $\mathrm{Tr}\mathbf{T}$) such that $\mathrm{Tr}\mathbf{T} = c_0^2 f(\epsilon/\epsilon_0)$, where f is some function to be determined experimentally and $f(1) = 1$, the diffusion equation may be written

$$\frac{\partial\tau}{\partial t} = \frac{2c_0^2}{r}\ \frac{\partial}{\partial r}\left\{\frac{1}{\Omega r}\ \frac{\partial}{\partial r}\left[r^2\tau\left(\frac{T_{r\theta}}{\mathrm{Tr}\mathbf{T}}\right) f(\epsilon/\epsilon_0)\right]\right\}. \tag{45}$$

The analytic, approximate expression for $T_{r\theta}/\mathrm{Tr}\mathbf{T}$ is given by Eq. (44). Since there is a relationship between ϵ and τ (see Eqs. 37 or 43), the right-hand side of the diffusion equation contains a function, say h, of τ and the two independent variables, r and t. It seems likely that $h(\tau)$ is a nonlinear function of τ so that Eq. (45) will not in general yield a linear diffusion equation. In particular, since $T_{r\phi}$ is a function of τ, its magnitude may change with time such that the time scale for radial spreading of a ringlet is not necessarily proportional to the square of the width of a ringlet as was assumed in the heuristic arguments presented in Sec. I.B.

The $\epsilon-\tau$ and $T_{ij}-\mathrm{Tr}\mathbf{T}$ relationships obtained in Sec. II.B.4 and the $\epsilon-\mathrm{v}_c$ relation to be determined experimentally may also be used to deduce a vertical scale height for the disk. In particular, from the observed τ we can determine a corresponding value of ϵ and then, from the $\epsilon-\mathrm{v}_c$ relationship, a value for v_c or equivalently $\mathrm{Tr}\mathbf{T}$. Using the numerical value of $\mathrm{Tr}\mathbf{T}$ in the energy equilibrium solution (Eq. 41), we deduce a value for T_{zz}, and thus a value for H ($\approx T_{zz}^{\frac{1}{2}}/\Omega$).

Although a $\epsilon-\mathrm{v}_c$ relationship is not yet available, we know that for most substances, very low-velocity collisions tend to be perfectly elastic. If the ring particles' ϵ remains unity up to an impact velocity v_1, there would be an absolute lower limit to the thickness of the rings such that $H \gtrsim H_1 = \mathrm{v}_1/\Omega$. A ring cannot be thinner than H_1 because the ring particles do not dissipate their dispersion velocity below the critical value which will support such a thickness. At large v_c, ϵ decreases with v_c. However, according to the energy-equilibrium solution of the second-order moment Eq. (37), the ring particles' ϵ cannot be smaller than 0.62, corresponding to $(1-b)^{\frac{1}{2}}$ for $\tau = 0$. Below this value of ϵ, the collisions are too dissipative to be able to sustain an energy equilibrium. If the experimentally-determined ϵ for the ring particles is reduced to $(1-b)^{\frac{1}{2}}$ at some velocity, say v_2, there would be an upper limit to the thickness such that $H \lesssim H_2 = \mathrm{v}_2/\Omega$. If, however, ϵ remains larger than $(1-b)^{\frac{1}{2}}$ for very larger values of v_c, there would be a limiting value in τ. A ring with a τ close to this limiting value can have a very large velocity dispersion such that the ring may be very thick and may evolve on a relatively short time scale. We show in Sec. IV that the disk is diffusively unstable for all τ in this case. The presence of regions of very low τ which are not influenced by external force fields such as resonant interactions with a satellite, will indicate that ϵ for the ring particles indeed reduces below $(1-b)^{\frac{1}{2}}$ at relatively small impact velocities.

The above discussions clearly indicate the importance of a theoretically determined $\epsilon-\tau$ law and the urgent need of an experimentally determined $\epsilon-\mathrm{v}_c$ law. In particular, the limiting value of ϵ for arbitrarily small τ and the values of ϵ for very small and very large v_c basically determine the vertical structure and the evolutionary fate of the rings. Recall that the $\epsilon-\tau$ law was derived from the second-order moment equation so that its actual prescription may be sensitive to the approximations used in evaluating the

collisional integral. In view of its importance and the numerous assumptions adopted for its evaluation, a more careful analysis of the $\epsilon-\tau$ relationship may be useful.

III. MATHEMATICAL FORMULATION: HYDRODYNAMICS

A. Basic Formulation

Although the kinetic treatment is designed to analyze rigorously the statistical properties of the particles in the ring, its complexity makes exact analytic solutions and their stability analyses unattainable. The above discussion is a clear indication that numerous approximations and simplifications are required to deduce and verify the most basic results. Overall, the mathematical complexity tends to obscure the central issue and the basic interpretation of the essential physical processes which dominate the structure, stability and evolution of the rings. However, to a considerable degree, these complexities may be reduced by the use of a fluid dynamical approximation. The essence of this approximation is that the dispersion velocity ellipsoid has a locally unique characteristic shape such that the pressure tensor may be divided into an isotropic part, represented by a scalar pressure, and a nonisotropic part represented by a stress tensor. The stress tensor is a product of locally determined transport coefficients, such as viscosity, and a globally determined shear tensor. This dependence on the global properties in the stress tensor is in contrast to the apparently total dependence on the local velocity dispersion ellipsoid in the pressure tensor in the kinetic treatment. As the analyses of the energy-equilibrium solutions of the second-order moment equations have already indicated, the pressure tensor is closely related to the global shear albeit indirectly. Through this approximation, all the complications associated with the evaluation of the dispersion-velocity ellipsoid are replaced by prescriptions for the transport coefficients. Consequently, the hydrodynamic equations have apparently somewhat simpler forms than the moment equations. In this case, the evolution of a ring may be determined from the hydrodynamical equations of continuity, momentum, and energy, which for a fluid of density ρ and velocity $\mathbf{u}$ can be written as

$$\frac{d\rho}{dt} + \rho \frac{\partial u_i}{\partial x_i} = 0 \tag{46}$$

$$\rho \frac{du_i}{dt} = -\frac{\partial P}{\partial x_i} - \rho \frac{\partial U}{\partial x_i} + 2 \frac{\partial}{\partial x_j} (\rho \nu e_{ij}) + \frac{\partial}{\partial x_i} \left[(\xi - \frac{2}{3} \nu) \rho \frac{\partial u_j}{\partial x_j} \right] \tag{47}$$

$$\frac{d}{dt} (\rho E) = -P \frac{\partial u_i}{\partial x_i} + 2 \rho \nu \left[e_{ij} e_{ij} - \frac{1}{3} \left(\frac{\partial u_i}{\partial x_i} \right)^2 \right]$$

$$+\rho\xi\left(\frac{\partial u_i}{\partial x_i}\right)^2+\frac{\partial}{\partial x_i}\left(\frac{\kappa\rho}{k_B}\frac{\partial E}{\partial x_i}\right)+\rho\dot{E}_c \tag{48}$$

where ν, ξ, and κ are the kinematic shear viscosity, bulk viscosity, and thermal conductivity, respectively, and $e_{ij} = 0.5(\partial u_i/\partial x_j + \partial u_j/\partial x_i)$ is the shear tensor. The pressure and internal energy (per unit mass) are denoted by P and E, respectively, and the rate of energy loss due to inelastic collisions is denoted by $\dot{E}_c$. The material time derivative, $\mathrm{d}/\mathrm{d}t$, contains both the local time derivative and the advective operator $(u_i\,\partial/\partial x_i)$ terms.

The leading terms of the somewhat simplified hydrodynamic equations have direct correspondence to leading contributions in the moment equations. From these corresponding terms, we may evaluate the magnitude and physical dependence of the transport coefficients. For example, after the vertical averaging, the continuity equation becomes

$$\frac{\partial\sigma}{\partial t}+\frac{1}{r}\frac{\partial}{\partial r}(r\sigma u_r)=0 \tag{49}$$

which is identical to the zeroth-order moment equation. Similarly, the leading terms in the momentum equation can also be identified with those in the first-order moment equation. In a thin, axisymmetric disk, the momentum equation has three components such that in cylindrical coordinates

$$\frac{\partial u_r}{\partial t}+u_r\frac{\partial u_r}{\partial r}-\Omega r^2=-\frac{GM}{r^2}-\frac{1}{\sigma}\frac{\partial P'}{\partial r}+\frac{2}{\sigma}\frac{\partial}{\partial r}\left(\sigma\nu\frac{\partial u_r}{\partial r}\right)$$

$$+2\nu\frac{\partial}{\partial r}\left(\frac{u_r}{r}\right)+\frac{1}{\sigma}\frac{\partial}{\partial r}\left[\sigma\left(\xi-\frac{2}{3}\nu\right)\frac{1}{r}\frac{\partial}{\partial r}(ru_r)\right] \tag{50a}$$

$$\frac{\partial}{\partial t}(\Omega r)+\frac{u_r}{r}\frac{\partial}{\partial r}(r^2\Omega)=\frac{1}{\sigma r^2}\frac{\partial}{\partial r}\left(\nu\sigma r^3\frac{\partial\Omega}{\partial r}\right) \tag{50b}$$

$$\frac{1}{\rho}\frac{\partial P}{\partial z}=-\frac{GMz}{r^3} \tag{50c}$$

where $P' = \int P\,\mathrm{d}z$ is the vertically integrated gas pressure. Equation (50c) is identical to the z component of the first-order moment equation if we identify P with mNT_{zz}. In our attempt to solve the moment equations, we have adopted an approximation in which T_{zz} is independent of z. This assumption corresponds to an isothermal equation of state in the hydrodynamic treatment. The solution for Eq. (50c) for an isothermal gas indicates that $N(z) = N(0)\exp[-z^2GM/(r^3 C_s^2)]$ where C_s is the sound speed; this

solution is, of course, identical to that obtained from the moment equations (see Eq. 29).

The analogy between Eqs. (50a) and (30) is more tenuous. Here, only the leading terms are identical whereas the interpretation of pressure, shear- and bulk-viscosity contributions is rather ambiguous. Fortunately, the contributions due to difficult-to-identify terms are negligibly small unless the disk flow is significantly noncircular for one of the following reasons: (1) the velocity dispersion on the ring is comparable to Ωr (or equivalently, the ring is very thick); (2) there is a very large pressure gradient in the radial direction due to sharp transitions; (3) there is a large bulk viscosity; and (4) the ring is strongly perturbed by external forces with very large radial gradients. In most regions of planetary rings these conditions are not realized so that Eq. (50a) is reduced to the standard prescription for Keplerian motion, $\Omega = (GM/r^3)^{\frac{1}{2}}$. However, near sharp edges of a typical ring, especially when the characteristic radial scale length is comparable to the vertical scale height, the ring flow may indeed become non-Keplerian and therefore it may be necessary to solve simultaneously the radial component as well as the θ-component of the equation of motion.

The θ-component of the equation of motion is useful for determining angular momentum transfer and mass flux in the radial direction. In those regions of the ring where particles follow Keplerian orbits Eq. (50b) becomes identical to Eq. (31) if we identify $T_{r\theta}$ with the quantity $-\nu r\partial\Omega/\partial r = 1.5\,\Omega\nu$. To dominant order, the radial mass flow becomes

$$\sigma u_r r = -\frac{3}{\Omega r}\frac{\partial}{\partial r}(r^2\Omega\,\sigma\,\nu)\ . \tag{51}$$

The equivalent to Eq. (34), the mass diffusion equation, also can be obtained with this substitution. This equation may be solved, for various initial conditions once a prescription for ν is specified. Equation (6) provides an order-of-magnitude estimate from the standard formula $\nu \simeq \omega_c \lambda^2$. A more rigorous derivation for ν may be obtained if we identify $1.5\,\Omega\nu$ with $T_{r\theta}$ as above and use the numerical results obtained by Goldreich and Tremaine (1978):

$$\nu = K_1 c^2\tau/[\Omega(1+\tau^2)] \tag{52}$$

where K_1 was calculated to be 0.15. An alternative expression for ν (Hämeen-Anttila 1978) is obtained from Eq. (44)

$$\nu = \frac{2[(19\epsilon - 13)(1-\epsilon)]^{\frac{1}{2}}\,\mathrm{Tr}\mathbf{T}}{9(3-\epsilon)\,\Omega} \tag{53}$$

and is in close agreement (see Sec. II.B.4). Furthermore, both relationships are closely analogous to an equivalent expression obtained by Cook and

Franklin (1964) who evaluated the collision integral with a Krook collision law. With the evaluation of these transport coefficients (or equivalently, different components of the pressure tensor), the mass diffusion equation may be solved numerically (or analytically under special circumstances) as an initial value problem once a relationship between τ and Tr$\mathbf{T}$ is established.

In a fluid approximation, the energy equation is analogous to the second-order moment Eq. (35). Direct comparison between these two equations can be made by identifying E with the kinetic energy associated with random motion i.e. Tr$\mathbf{T}$. The term $\partial(\rho E)/\partial t$ represents the rate of change in kinetic energy associated with the random motion which is analogous to $\partial(\sigma \mathrm{Tr}\mathbf{T})/\partial t$. The term $P\ \partial u_i/\partial x_i$ is the energy contribution due to P dV work and is equivalent to the $P_{ij}\ \partial u_k/\partial x_k$ term. Viscous dissipation processes, described by the second and third terms on the right-hand side of Eq. (48), induce an energy transfer from the systematic shearing motion into the random motion and are related to the $P_{jk}\ \partial u_i/\partial x_k$ terms. The local heat flux due to conduction $\partial(\kappa\rho\ \partial E/\partial x_i)/\partial x_i$ is equivalent to the term $\partial p_{ijk}/x_k$. Finally, an energy loss rate, $\dot{E}_c$, is incorporated to account for the rate of energy loss due to inelastic collisions which is described by $(\partial p_{ij}/\partial t)_c$ in the kinetic theory approach. There is no simple way to estimate $\dot{E}_c$ without carrying out the evaluation of the collisional integral as we have done in the kinetic treatment presented in Sec. II.B.2. Therefore we shall utilize this result by setting $\dot{E}_c = K_2\ (1-\epsilon^2)\ \tau\ c^2\ \Omega$, where K_2 is a constant of order unity, in analogy with Eq. (11). If we compare this expression with the rigorous calculations referred to in Sec. II.B.3, we find that K_2 has a value ranging from 0.9 to 1.5, depending on the method of evaluation of the collisional integral. For convenience, we set $K_2 = 1$.

The energy equation for a thin disk may be written in cylindrical coordinates as follows:

$$\frac{\partial E}{\partial t} + u_r \frac{\partial E}{\partial r} + \left(\frac{\Gamma_3 - 1}{r}\right)\frac{\partial}{\partial r}(u_r r) = \frac{9}{4}\nu\,\Omega^2 - (1-\epsilon^2)\,\tau\,c^2\,\Omega$$

$$+ \frac{1}{r}\ \frac{\partial}{\partial r}\left(\frac{\kappa}{k_B}\ \frac{\partial E}{\partial r}\right) \tag{54}$$

where Γ_3 is the third adiabatic exponent. If the disk is smoothly varying, contributions due to the advective transport, PdV work, and thermal conduction are negligible compared with the energy generation process associated with viscous stress and energy dissipation due to inelastic collision.

Thus, in equilibrium, the energy equation becomes

$$\frac{9}{4}\nu\,\Omega^2 = (1-\epsilon^2)\,\tau\,c^2\,\Omega\ . \tag{55}$$

This equation is entirely analogous to Eq. (40). From Eq. (52) it follows that $(1 + \tau^2)(1-\epsilon^2) = 0.6$. Substituting this $(\epsilon-\tau)$ relation, Eq. (51) and Eq. (52) into the continuity Eq. (49) and using $\tau = \pi R_p^2 \sigma/m$, we obtain a mass diffusion equation,

$$\frac{\partial \tau}{\partial t} = \frac{3K_1}{r} \frac{\partial}{\partial r}\left\{\left(\frac{1}{\Omega r}\right)\frac{\partial}{\partial r}\left[\frac{\tau^2 r^2 c^2}{(1+\tau^2)}\right]\right\} \tag{56}$$

where c is a function of ϵ and therefore of τ. Equation (56) is analogous to the corresponding Eq. (45) obtained from the kinetic approach.

B. The Energy Budget of Accretion-Disk Flow

Since ring particles undergo frequent inelastic collisions, the energy E associated with dispersive motion is continually drained from the system. This internal energy, in turn, is continually supplied by the kinetic energy of orbital motion via viscous stress. Ultimately, the kinetic energy must be replenished by the release of gravitational energy associated with a net inward drift of the ring particles. This general, qualitative description of the basic energy-flow pattern in a differentially rotating accretion disk, such as a planetary ring, may be examined rigorously with a fluid-dynamical approach which was first adopted by Lynden-Bell and Pringle (1974).

We begin by considering the rate of change of potential and kinetic energy carried by a fluid element with a fixed increment of mass dm and a variable physical volume, $dV = dm/\rho$. We first multiply u_i by the momentum Eq. (47), then add the result to the product of u_i and the continuity equation, and then integrate over dV such that

$$\frac{d}{dt}\int_V \left(\frac{u^2}{2} + U\right) dm = \int_V u_i \frac{\partial}{\partial x_j}\left[-P\delta_{ij} + 2\rho\nu e_{ij} + \rho\left(\xi - \frac{2}{3}\nu\right) e_{kk}\,\delta_{ij}\right] dV. \tag{57}$$

In the derivation of the above equation, we have assumed $\partial U/\partial t = 0$. With the use of the divergence theorem, the above equation for a thin disk between radii r_1 and r_2 becomes

$$\frac{d}{dt}\int_V \left(\frac{u^2}{2} + U\right) dm = \left[-2\pi r u_r P' + 2\pi\sigma\nu r^3 \Omega\, \partial\Omega/\partial r\right]_{r_1}^{r_2} - \int_{r_1}^{r_2} 2\pi r^3 \nu\sigma \left(\frac{\partial\Omega}{\partial r}\right)^2 dr + \int_V P \frac{d}{dt}\left(\frac{1}{\rho}\right) dm \tag{58}$$

The left-hand side of the above equation represents the rate of change in kinetic and gravitational energy associated with ring material flowing into the potential well of the central planet. On the right-hand side, the first term represents the flux of internal energy advected into the region under consideration by the bulk motion of the ring particles. The second term is the rate of kinetic-energy transfer by viscous coupling. Note that even in the absence of any bulk motion, this viscous coupling can still provide an effective energy transfer across the disk. While potential energy may be converted into kinetic energy in one region of the ring, e.g., via spreading of the ring at the inner and outer boundaries, viscous coupling effects may cause the newly transformed kinetic energy to be transferred into another region. In fact, both of the first two terms are associated with global properties at the boundaries. They represent energy redistribution processes. The third term is associated with the rate of energy transfer, from kinetic into internal energy, due to viscous stress. Note that both the second and third terms depend only on the kinetic shear viscosity but not on the bulk viscosity. Thus, in a uniformly rotating disk, the local shear reduces to zero so that these terms vanish. Also of importance to this contribution is the presence of a nonvanishing frictional effect. The fourth term is associated with the rate of change in the internal energy associated with PdV work. Both the third and fourth terms are referring to local effects. They represent the conversion between internal and kinetic energy. Actually, the last two terms may be replaced with a term corresponding to the rate of change of internal energy. If we integrate the internal energy Eq. (48) with respect to dV and then add it to Eq. (57) we obtain

$$\frac{d}{dt}\int_V \left(\frac{u^2}{2} + U + E\right) dm = \int\left[-P\delta_{ij} + 2\nu\rho e_{ij} + \rho\left(\xi - \frac{2}{3}\nu\right)\frac{\partial u_k}{\partial x_k}\delta_{ij}\right] u_i dS_j$$

$$+ \int \frac{\rho\kappa}{k_B}\frac{\partial E}{\partial x_i} dS_i + \int_V \dot{E}_c\, dm$$

$$= [-2\pi r u_r P' + 2\pi\sigma\nu r^3 \Omega\partial\Omega/\partial r]_{r_1}^{r_2} + \int_{r_1}^{r_2} \frac{\sigma k}{k_B}\frac{\partial E}{\partial r} dr + \int E_c\, dm \qquad (59)$$

where the integration variable S refers to the surface of a cylinder concentric with the axis. Although the rate of change of internal energy, due to motion in the potential well of the planet, on the left-hand side of Eq. (59) has replaced terms three and four on the right-hand side of Eq. (58), the internal and kinetic energy can still be transferred by advective and viscous-coupling effects, respectively. In addition, the internal energy may be redistributed in a ring by collisionally induced conduction. The internal energy is drained by inelastic collisions.

The above equation clearly indicates that the loss of internal energy, by inelastic collisions, at any region of the ring is roughly balanced by a local gain in which the viscous stress transforms kinetic energy into internal energy. The loss of kinetic energy may be countered by global transport processes which redistribute the kinetic energy from elsewhere. The overall energy flow is maintained by the ring's motion into deeper parts of potential well of the planet. This characteristic can be best appreciated in the limit of small E and κ where only the viscous coupling and the inelastic collision terms are of importance. It is their balance which determines the evolutionary fate of the ring.

Under certain specialized conditions it is possible for a disk to evolve to a quasi-steady state in which the local time derivatives are small (Lynden-Bell and Pringle 1974; Lin and Bodenheimer 1982). From the continuity Eq. (49) we find that $\dot{m} = 2\pi\sigma u_r r$ is independent of r. Thus we may integrate the θ-component of the momentum Eq. (50b) to obtain

$$\sigma u_r r^3 \Omega = \sigma \nu r^3 \, \partial\Omega/\partial r + \dot{J}_c/2\pi \ . \tag{60}$$

The integration constant $\dot{J}_c$ may be interpreted as the Lagrangian angular-momentum flux across any radius. Although $\dot{J}_c$ is independent of r, it is a linear combination of two radially-varying functions: an outwardly directed angular-momentum flux induced by viscous transfer and an inwardly directed Eulerian angular momentum flux carried by the inwardly drifting particles. Note that we have defined $\dot{m}$ and $\dot{J}_c$ in such a manner that negative values imply mass and angular momentum transfer onto the planet. At the inner boundary of a freely expanding ring there is no viscous coupling so that $\dot{m}$ and $\dot{J}_c$ would have the same sign. Alternatively it may be possible to maintain a planetary ring in a steady state, in which $\dot{m} = 0$, by a strong viscous coupling at the rings' two boundaries. Such coupling may be caused by a variety of physical processes such as tidal effects from shepherding satellites or a boundary-layer interaction between the ring and the accreting planet. In this case, the energy loss due to inelastic collision is continually supplied by the viscous coupling process. For a ring with a finite mass flux, the particles steadily drift inward with a radial velocity

$$u_r = \frac{\nu}{r} \frac{\partial \ln\Omega/\partial \ln r}{\left(1 - \dfrac{\dot{J}_c}{\dot{m}\,\Omega r^2}\right)} . \tag{61}$$

Away from boundaries of the ring, the quantity $\dot{J}_c/(\dot{m}\Omega r^2)$ is usually positive and much smaller than unity so that in a Keplerian disk $u_r = -3\nu/2r$.

In the quasi-steady state the physical significance of the dominant terms in the energy equation is vividly demonstrated. In this case

$$\frac{d}{dt}\int_V\left(\frac{u^2}{2}+U+E\right)dm=\int 2\pi r\,\sigma u_r\frac{\partial}{\partial r}\left(\frac{u^2}{2}+U+E\right)dr$$
$$=\dot{m}\left[\frac{u^2}{2}+U+E\right]_{r_1}^{r_2} \tag{62}$$

so that Eq. (59) becomes

$$\dot{m}\left[\frac{u^2}{2}+U+E\right]_{r_1}^{r_2}=[2\pi r^3\sigma\nu\Omega\partial\Omega/\partial r]_{r_1}^{r_2}+\int_V\dot{E}_c\,dm \tag{63}$$

where we have neglected the PdV work and the thermal conduction terms. The viscous coupling contribution (first term on the right-hand side of Eq. (63) may be expressed in terms of the mass flow,

$$[2\pi r^3\sigma\nu\Omega\,\partial\Omega/\partial r]_{r_1}^{r_2}=[\dot{m}\Omega^2r^2]_{r_1}^{r_2}=[\dot{m}\,u^2]_{r_1}^{r_2} \tag{64}$$

to show that it is twice the contribution arising from the orbital kinetic energy of the inwardly drifting particles. Thus, Eq. (63) becomes

$$[\dot{m}E]_{r_1}^{r_2}=\left[\frac{3}{2}\,\dot{m}\,\Omega^2r^2\right]_{r_1}^{r_2}+\int_V\dot{E}_c\,dm\,. \tag{65}$$

Since the difference in internal energy ($E=c^2/2$) between r_1 and r_2 is small, Eq. (65) indicates a balance between internal energy growth caused by viscous evolution and internal energy damping by collisions. The total orbital energy difference between particles at r_1 and r_2 is

$$\left[\frac{1}{2}u^2+U\right]_{r_1}^{r_2}=-\left[\frac{1}{2}\,\Omega^2r^2\right]_{r_1}^{r_2} \tag{66}$$

which is three times smaller than the power liberated between radii r_1 and r_2. The balance is supplied by the energy transport due to the viscous couple (Lynden-Bell and Pringle 1974). This simplified steady-state analysis clearly illustrates the energy redistribution processes that occur in a viscously evolving particle disk. Qualitatively, a similar energy redistribution process must occur in general nonsteady-state disks.

IV. THERMAL AND VISCOUS STABILITY OF A PLANETARY RING

There are three important reasons for examining the hydrodynamic stability of a planetary ring:

1. Both the moment equations in the kinetic theory and the transport equations in fluid dynamics are established on the basis of the hydrodynamic approximation that radial gradients are small. As we have indicated in Sec. I.B.2, in order to justify this approximation, there must exist a basic fluid element within which the ring particles' dynamics may be studied collectively. This justification may be rigorously satisfied by a demonstration that the ring is indeed stable against perturbations with wavelength comparable to H.
2. The derivation of transport coefficients, such as viscosity, is based on an energy-equilibrium assumption. In order for this assumption to be satisfied, a planetary ring must be thermally stable, i.e., it can return to a state of energy-equilibrium, through inelastic collisions and viscous stress, after a small perturbation is imposed. Although we have already qualitatively outlined a condition for thermal stability in Sec. I, a rigorous stability analysis is still worthwhile.
3. The steady-state assumption produces an optical depth which varies smoothly with r, i.e., $d \ln \tau / d \ln r$, should be of order unity. However, Voyager data on Saturn's rings indicate that the ring system is divided into thousands of ringlets in which the optical depth varies rapidly with radius. Although some of the gaps and ringlets may be caused by resonant interactions with Saturn's numerous inner satellites (see chapters by Shu and by Franklin et al.), many features seem to be intrinsic to the ring's internal dynamics. One possible interpretation of the phenomenon is that it is caused by a viscous instability somewhat analogous to the traffic jam problem. This possibility may be verified with a rigorous stability analysis.

The above three issues may be addressed with different degrees of sophistication. The third issue, i.e., the origin of ringlets, may be most simply addressed with a viscous-stability analysis based on a perturbation calculation of the mass diffusion equation. The second issue requires a simultaneous perturbation analysis of the mass as well as energy transport equations whereas the first requires, in addition, a perturbation analysis of the momentum equations. We shall discuss these issues in order of increasing sophistication, i.e., in reverse order. In Sec. IV.A.3. we also give a qualitative discussion of the physical mechanisms which give rise to diffusion instabilities and contrast them with the earlier ideas of jet-stream formation.

A. Viscous Stability of Planetary Rings and the Origin of the Ringlets

The first stability analysis is to be carried out with the simplest possible approach, which is somewhat analogous to that performed by Lightman and Eardley (1974) in a different astrophysical context. In this analysis, the ring is assumed to always be in a state of energy-equilibrium so that (1) there is a $\epsilon - \tau$ relationship (see Eq. 37) and (2) ν may be expressed in the form

of Eq. (52). Both assumptions may be justified later with a thermal stability analysis provided ϵ decreases with v_c. Since an $\epsilon - v_c$ relationship is not yet available, we adopt the *ad hoc* assumption $c \propto \sigma^{\delta}$ and investigate both analytically and numerically, under what conditions the system is stable.

1. An Analytic Stability Treatment. For computational convenience, the physical dimensions in the diffusion equation may be eliminated by use of the variable $\xi = r/r_0$ where r_0 is taken to be the point of unit optical depth, i.e., $\tau(r_0) = \tau_0 = 1$. Thus $\sigma/\sigma_0 = \tau$ where $\sigma_0 = \sigma(r_0)$. Now let $X = \xi^{\frac{1}{2}}$ and $T = t\Omega_0/R$ where $\Omega_0 = \Omega(r_0)$ and $R = \Omega_0 r_0^2/\nu_0$ is the Reynolds number; then Eq. (56) reduces to

$$\frac{\partial \tau}{\partial T} = \frac{3K_1}{X^3} \frac{\partial^2}{\partial X^2} \left[X^4 \tau^{2\delta} (1 + \tau^{-2})^{-1} \right] . \tag{67}$$

Following standard procedures in linear stability analyses, we introduce a small-amplitude, short-wavelength, sinusoidal perturbation τ_2 upon a general solution τ_1, in the neighborhood of some radius r_1, so that

$$\tau(X,T) = \tau_1(X,T) \left[1 + \tau_2(X,T) \right] \tag{68}$$

where

$$\tau_2 = A e^{-sT} \sin k(X - X_1) . \tag{69}$$

By assumption, we may choose $A << 1$ and $kX_1 >> 2\pi$, where the dimensionless perturbation wavelength is $\lambda/r = 2\pi/k$. The criteria for choosing the appropriate limits for wavelength are (1) it should be sufficiently short so that the mass-diffusion equation may be linearized, and (2) it should be sufficiently long so that the pressure-gradient effects, on momentum and energy transport, remain negligibly small.

Introducing Eqs. (68) and (69) into (67) and neglecting terms second-order in A, we obtain

$$s = 6k^2 \left[\delta + (1 + \tau_1^2)^{-1} \right] X \tau_1^{2\delta} / (1 + \tau_1^2) . \tag{70}$$

Equation (70) indicates that $s > 0$ for $\delta > 0$ and therefore these disks are stable and perturbations on them are always damped. For $\delta < -1$, s is always negative and perturbations would grow if the $c \propto \sigma^{\delta}$ law remains valid. For $-1 < \delta < 0$, s is positive if $\tau < \tau_c = [-(1+\delta)/\delta]^{\frac{1}{2}}$ and negative if $\tau > \tau_c$. Provided $-1 < \delta < 0$ we would expect the instability to develop into regions of very high optical depth, separated by gaps with optical depth $\leq \tau_c$, since these regions are stable. Note, however, if $\delta < -1$, all regions of the disk are

unstable, whether optically thin or optically thick. One would expect the instability to develop into regions of alternately very high or very low τ.

The above linear stability analysis was based on work by Lin and Bodenheimer (1981). A similar analysis was performed by Ward (1981), who found the essentially equivalent criterion that instability occurs if

$$\frac{\partial}{\partial \sigma}(\nu\sigma) < 0 \, . \tag{71}$$

Assuming that the viscosity coefficient is given by Eq. (52) with $K_1 = 0.15$ and the coefficient of restitution is related to c by $(1-\epsilon^2) \propto (c^2)^{1/\alpha}$, where α is expected to be fairly large, he finds that criterion (71) is satisfied if $\tau > \tau_c = \alpha^{-\frac{1}{2}}$. Thus, if τ is larger than some critical value of perhaps 0.3 to 0.5, instability occurs. Note that this $\epsilon - c$ relation replaces the assumption $c \propto \sigma^{\delta}$ used by Lin and Bodenheimer.

2. *Numerical Confirmation.* The occurrence of the instability can be verified and studied in more detail by the use of numerical techniques which can follow the evolution into the nonlinear regime. Such models have been presented by Lin and Bodenheimer (1981) with fluid-dynamical techniques and by Lukkari (1981) with N-body particle techniques. Lin and Bodenheimer (1981) consider the full time-dependent nonlinear solution of Eq. (67). This diffusion equation for τ has the same general form as the simple heat conduction equation which can be solved, as described by Richtmyer (1957), by an implicit numerical technique. The initial conditions were taken to be steady-state solution calculated under the assumption that $c \propto \sigma^{\delta}$, modified by short-wavelength sinusoidal perturbations in τ of the form for Eq. (69). Parameters investigated included δ, wave number k, amplitude A, and location X_1. Typical examples of stable and unstable solutions are given in Figs. 5 and 6. In all cases investigated, the stability criterion deduced from Eq. (70) was verified. Since no cutoff on the $c \propto \sigma^{\delta}$ law was imposed, perturbations grew indefinitely in the unstable regime. In the region where $-1 < \delta < 0$, the surface density decreased, in the regions where it was initially perturbed downwards, until $\tau = \tau_c$, as expected from the stability condition. Although the calculations could not be continued beyond one e-folding time, because numerical perturbations of very short wavelengths began to grow rapidly, some calculations were carried into the nonlinear regime by a choice of a relatively large initial value for A. In these cases also, there was good agreement between the numerical results and the linear stability analysis.

The growth time for the instability can be deduced from the quantity s (Eq. 70) and the scaling relation for T. The result is

$$t_g \simeq \frac{R\tau}{3Xk^2\Omega} \simeq \frac{R\lambda^2\tau}{r^2\Omega} \, . \tag{72}$$

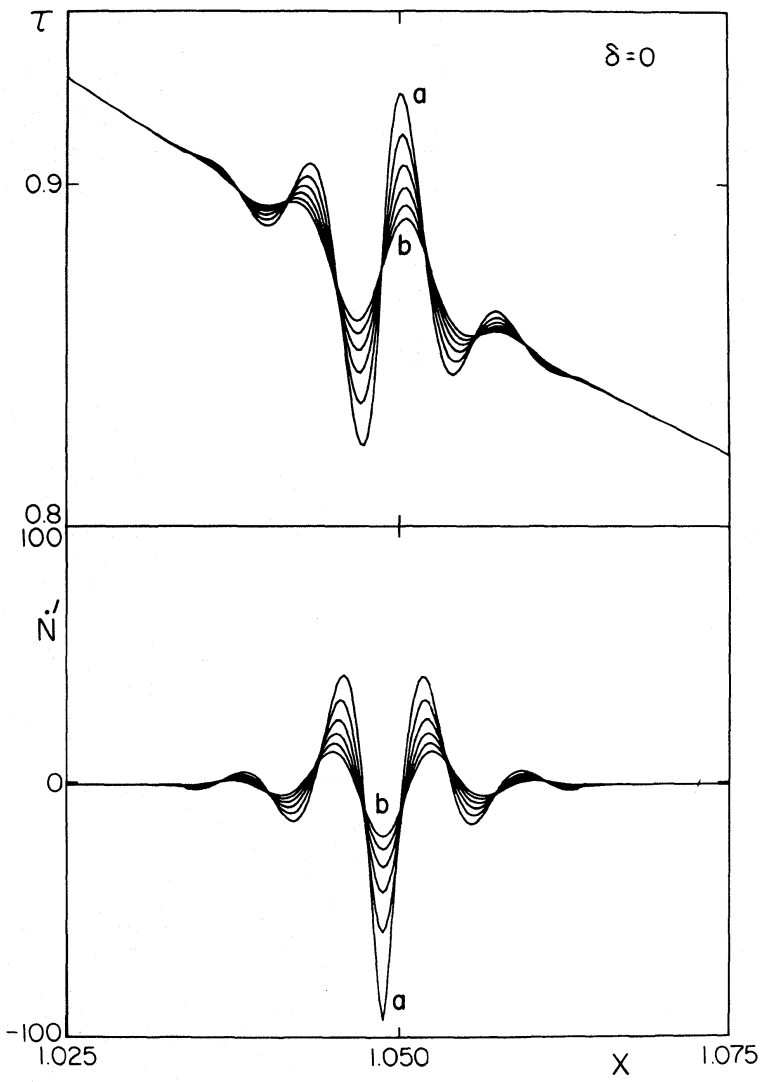

Fig. 5. The decay of a perturbation on a stable steady-state disk for $\delta = 0$, $X_1 = 1.05$, $A = 0.07$, and $k = 8.4 \times 10^2$ (see Eq. 69). *Upper portion*, optical depth; *lower portion*, normalized mass transfer rate $\dot{N}' = \dot{N}/(3\pi\sigma\nu)$ where $\dot{N}$ is calculated from Eq. (75). The six curves are separated by equal time intervals starting with initial condition (a) and ending after one e-folding time (b). Numerical simulations are from Lin and Bodenheimer (1981).

The diffusion time for the overall spreading of the disk (Lynden-Bell and Pringle 1974) is $t_d \approx R\,\Omega^{-1}$. The simple argument that t_d must be $> 5 \times 10^9$ yr yields the condition $R \gtrsim 3 \times 10^{13}$. Thus for ringlets with wavelength 100 km, $t_g \geqslant 10^4 \tau$ yr. Alternatively, by setting $R \cong \Omega_0 r_0^2/\nu_0$ we obtain $t_g \simeq \lambda^2/\nu_0$, thus for $\lambda = 100$ km and measured estimates for $\nu \approx 260$ (Lissauer et al. 1983; chapters by Shu and by Cuzzi et al.) the growth time is $\sim 10^4$ yr at $\tau = 1$. The numerical results give very good agreement with these estimates from the linear stability analysis. Note that there is no preferred length scale for the instability; however, the growth time decreases sharply with decreasing wavelength.

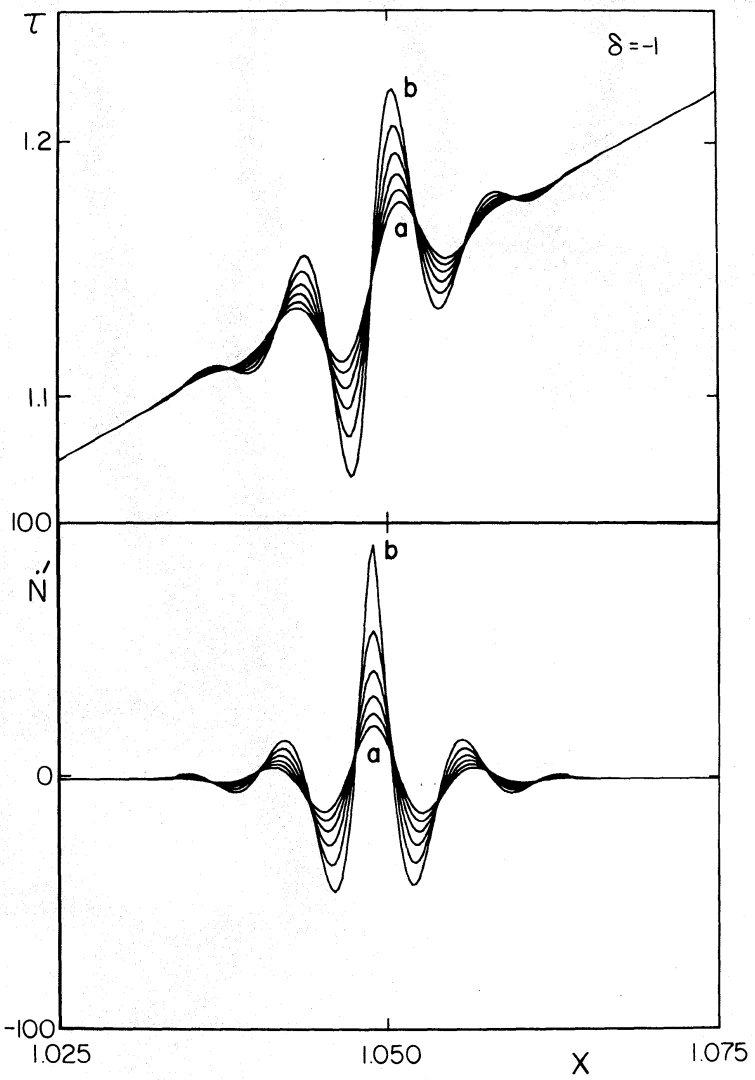

Fig. 6. The growth of a perturbation on an unstable steady-state disk for $\delta = 1$, $X_1 = 1.05$, $A = 0.06$, and $k = 8.4 \times 10^2$. The symbols and the source of the figure are the same as for Fig. 5.

An alternative time-scale estimate can be obtained from the linear stability analysis of Ward (1981):

$$t_g \simeq 5.4 \times 10^3 \left(\frac{\lambda_2}{H'}\right)^2 \frac{(1+\tau^2)^{2+\alpha}}{(\alpha\tau^2 - 1)} \text{ yr} . \tag{73}$$

Here $\lambda_2 = \lambda/500$ km where λ is the wavelength and $H' = H_0/10$ m where H_0 is the scale height at zero optical depth. For typical values ($\lambda_2 = H' = 1$) at optical depth 1, $t_g = 10^5$ yr for $\alpha = 3$ and 10^6 yr for $\alpha = 10$. Thus for $\lambda_2 = 100$, $t_g = 4 \times 10^3$ yr and 4×10^4 yr, respectively, in reasonable agreement with the results from Lin and Bodenheimer and much shorter than the age of the solar system.

A second approach to the numerical problem was carried out by Lukkari (1981) who explicitly calculated the evolution arising from collisions of a system of 250 orbiting particles. The coefficient of restitution was assumed to obey the condition.

$$\epsilon = \left[1 + K(\tau^3 + \tau_a^3)c\right]^{-1} \tag{74}$$

where K and τ_a are constants. With this relation, instability sets in for $\tau \geqslant 0.75$. An initially assumed broad density maximum in a small interval of distance from the planet increased in amplitude by a factor of 4 and evolved into a narrow spike after 33,000 collisions. This amplification of the density confirmed earlier analytical work on collisional Keplerian disks by Hämeen-Anttila (1978) who apparently was the first to predict that such amplification could occur and that one might expect the Saturn ring system to be broken up into ringlets. An analogous instability had been investigated earlier in the context of gaseous accretion disks around neutron stars and black holes where turbulent viscosity is responsible for angular momentum transport and radiation pressure plays an important role (Lightman and Eardley 1974; Shakura and Sunyaev 1976).

3. Physical Explanation for the Instability. On a Keplerian particle disk the collisions normally induce a viscous stress such that mass transfer occurs with a flux

$$m\dot{N} = \frac{-2}{\Omega r}\frac{\partial g}{\partial r} \tag{75}$$

where $g = 3\pi\Omega r^2 \nu\sigma$ is the viscous couple (Lynden-Bell and Pringle 1974). In the case of quasi-steady state, $\sigma\nu$ is constant so that $\dot{N}$ is a negative constant and the direction of mass flow is inward. However, in an unstable disk this assumption is not valid and the direction of mass transfer depends on the sign of $\partial g/\partial r$. It turns out that the local mass flow is towards a local density maximum from both directions. To see this, write

$$m\dot{N} = \frac{-2}{\Omega r}\frac{\partial g}{\partial \sigma}\frac{\partial \sigma}{\partial r}. \tag{76}$$

If, in a density perturbation, σ increases outwards, the mass flow is outwards (toward the σ-maximum) if $\partial g/\partial\sigma < 0$. Similarly, if σ increases inwards in the perturbation, the mass flow is inwards (again towards the density maximum) if $\partial g/\partial\sigma < 0$.

To examine the sign of $\partial g/\partial\sigma$ more carefully, we assume, as above that $c \propto \sigma^{\delta}$ and we consider a short-wavelength perturbation $\lambda << r$. Then we can write

$$\frac{\partial g}{\partial \sigma} \propto \frac{\partial}{\partial \sigma}\left[\sigma^{2\delta}(1+\tau^{-2})^{-1}\right] . \tag{77}$$

Clearly, if $\delta < 0$ and $\tau > 1$, the disk is unstable since $\partial g/\partial \sigma < 0$, and if $\delta < -1$ it is unstable for $\tau << 1$, since $\partial g/\partial \sigma \propto 2\,(\delta+1)$. Note that the stability criterion is modified for small τ in this model, and in the models of Ward and Lukkari it does not occur at all for τ less than some critical value.

The numerical diffusion calculations (Figs. 5 and 6) illustrate the direction of mass flow. For the stable solution, in the region where σ increases outwards $\dot{N}$ is sharply negative, that is, viscosity tends to decrease the amplitude and spread out the perturbation. Similarly, where σ decreases outward, $\dot{N}$ is positive, away from the density maximum. On the other hand, in the unstable case where $\partial\sigma/\partial r > 0$, $N > 0$ so the density enhancement is reinforced. Similarly when $\partial\sigma/\partial r < 0$, $N < 0$ and mass transfer again is toward the density maximum.

In summary, the criterion that determines whether a particle disk spreads or clumps depends on the relationship between velocity dispersion and surface density, since this relationship controls the form of the viscous stress given in Eq. (77). Our assumption of energy equilibrium also establishes a relationship between τ and ϵ (Eq. 37). Thus, the criterion for diffusion instability ultimately depends on how ϵ varies with the velocity dispersion. The fact that ϵ is a decreasing function of velocity does not guarantee a diffusion instability; the stability criterion depends in a complicated way on the particular form of the $\epsilon - v_c$ relation. For the particular power-law relation assumed by Ward (1981), $(1-\epsilon^2) = K(c^2)^{1/\alpha}$, the exponent $1/\alpha$ determines the critical optical depth above which there is instability. If α were too small, the instability would require an impossibly large τ.

It should be emphasized that our explanation of the diffusion instability is fundamentally a *fluid* description caused by a stress imbalance between neighboring fluid elements of particles. It has yet to be rigorously described by a kinetic theory (see Sec. IV.B.2). The diffusion instability is distinctly different from Alfvén and Arrhenius' (1976) "jet stream" hypothesis. They argue that the inelasticity of collisions would dissipate relative motion to such an extent that particle orbits would cluster into a narrow stream with correlated orbital elements (i.e., arguments of pericenter and ascending nodes as well as semimajor axes would cluster). This idea does not require a particular $\epsilon - v_c$ relation; only that collisions be very inelastic. Indeed, their scenario seems to require an initial state out of energy equilibrium such that the excess velocity dispersion can be efficiently damped during the jet-stream formation process. In contrast, the diffusion instability can start from a state of energy equilibrium. Baxter and Thompson (1973) attempted to verify the jet-stream hypothesis with a kinetic theory, but their favorable conclusions are based on overly restrictive assumptions for the distribution of orbital elements and their relative rates of change. Trulsen (1972*b*) succeeded in demonstrating jet-

stream formation in a 2-dimensional N-body simulation, but only for an extremely dissipative collision model (see Sec. II.A). Hämeen-Anttila and Lukkari (1980) found a suggestion of a jet-stream effect in a 3-dimensional hard-sphere simulation only when they assumed a restitution coefficient ϵ that was too small (~ 0.25) to allow an energy equilibrium to be established (see Fig. 2). Under realistic conditions in planetary rings, it seems unlikely that the jet-stream mechanism plays an important role.

B. Intermediate-Wavelength Thermal and Viscous Stability Analysis.

The above viscous stability analysis is based on the assumption that the ring is always in a state of energy equilibrium. We now derive the conditions under which this assumption may be satisfied.

1. The Fluid Approximation. The thermal stability of an accretion-disk flow is closely related to the viscous stability (Shakura and Sunyaev 1976). In the stability analysis, a perturbation must be introduced to offset the delicate energy balance between inelastic collisions and viscous stress. As in Sec. IV.A, we concentrate our attention on intermediate wavelength perturbations for simplicity. In principle, the stability analysis should be carried out with the kinetic approach since such a perturbation may distort the general shape of the dispersion-velocity ellipsoid. The evolution of individual elements of the pressure tensor can only be obtained through the 3 components of the second-order moment Eq. (19) and the mass diffusion equation. In practice, the most important aspects of the stability analysis, namely the evolution of perturbations on σ and $\mathrm{Tr}\mathbf{T}$, may be carried out with a fluid-dynamical approach. In this case, perturbations are imposed on τ and $E = c^2/2$ such that

$$\begin{aligned} \tau &= \tau_1 (1 + \tau_2 e^{\lambda \tau} \sin kr) \\ E &= E_1 (1 + E_2 e^{\lambda \tau} \sin kr) \end{aligned} \tag{78}$$

where τ_1 and E_1 are the initial value of τ and E at r_1. The evolution of these perturbations may be analyzed with the mass diffusion Eq. (56) and the energy Eq. (54). In this analysis, a prescription for ν of the form

$$\nu = \frac{2K_1 E \tau}{(1+\tau^2)\,\Omega} \tag{79}$$

may be adopted (see Eq. 52). Such a viscosity law may be justified, even in a perturbed state, by the heuristic arguments in Sec. I. In essence, only the

effects of Tr$\mathbf{T}$ and τ on ν are included whereas the effect of the distortion of the dispersion-velocity ellipsoid has been neglected. The equations then become

$$\frac{\partial \tau}{\partial t} = \frac{6K_1}{\sqrt{GM}} \frac{1}{r} \frac{\partial}{\partial r}\left[r^{\frac{1}{2}} \frac{\partial}{\partial r}\left(\frac{E\tau^2 r^2}{1+\tau^2} \right) \right] \tag{80}$$

$$\frac{\partial E}{\partial t} = E\tau\Omega \left[\frac{9}{4} \frac{2K_1}{(1+\tau^2)} - (1-\epsilon^2) \right]. \tag{81}$$

For intermediate wavelength perturbations, these equations retain all the important terms for mass, angular momentum and energy transport.

We start the stability analysis with an initial condition that the ring is in a state of energy equilibrium such that τ_1 and E_1 at some radius r_1 obey the normal $\epsilon-\tau$ relationship for energy equilibrium (Eq. 37). The linearized resulting equations become

$$\lambda\tau_2 + \frac{6K_1 k^2}{\Omega}\left[\frac{2\tau E}{(1+\tau^2)^2}\tau_2 + \frac{\tau E}{(1+\tau^2)} E_2 \right] = 0 \tag{82}$$

$$E_2\left(\lambda - \tau\Omega E \frac{\partial \epsilon^2}{\partial E} \right) + \frac{9K_1 \tau^3 \Omega \tau_2}{(1+\tau^2)^2} = 0 .$$

These two simultaneous equations for E_2 and τ_2 can be solved to give

$$\lambda^2 + A\lambda + B = 0 \tag{83}$$

$$\text{where } A = \frac{12K_1 k^2 \tau E}{\Omega(1+\tau^2)^2} - \tau\Omega E \frac{\partial \epsilon^2}{\partial E} \tag{84a}$$

$$\text{and } B = \frac{-12K_1 k^2 \tau^2 E^2}{(1+\tau^2)^2}\left(\frac{\partial \epsilon^2}{\partial E} \right) - 54 \frac{K_1^2 k^2 \tau^4 E}{(1+\tau^2)^3} . \tag{84b}$$

The two roots are

$$\lambda_{\pm} = \frac{-A \pm \sqrt{A^2 - 4B}}{2} . \tag{85}$$

The negative root corresponds to thermal stability if $A^2 > 4B$ (which a little algebra shows is always true) and $A > 0$. Thus, thermal stability is guaranteed as long as $\partial\epsilon^2/\partial E < 0$ while thermal instability occurs ($A < 0$) if the condition

$$k^2 < \frac{\Omega^2 (1+\tau^2)^2}{12 K_1} \frac{\partial \epsilon^2}{\partial E} \tag{86}$$

is satisfied, which is impossible unless $\partial \epsilon^2 / \partial E > 0$.

The positive root corresponds to viscous instability if $\lambda_+ > 0$, which occurs if $A > 0$ and $B < 0$. The first condition is satisfied if $\partial \epsilon^2 / \partial E < 0$ so that the disk is thermally stable. In that case we can employ the condition for collisional equilibrium:

$$\frac{9}{2} \frac{K_1}{(1+\tau^2)} = (1 - \epsilon^2) \, . \tag{87}$$

Substituting this expression into the equation for B, we obtain the instability criterion

$$E \frac{\partial \epsilon^2}{\partial E} + (1 - \epsilon^2) \tau^2 > 0. \tag{88}$$

Thus the analysis gives the conditions for both viscous and thermal instability, and Eq. (88) defines a general relation between ϵ, c, and τ that is required for the occurrence of a viscous diffusion instability. Given a relation between ϵ and τ, this expression provides an estimate of the minimum value of τ that is required for instability. Setting the left-hand side of Eq. (88) equal to zero, substituting Eq. (37) and plotting the resulting curve in Fig. 7, we find that the $(\partial \ln \epsilon / \partial \ln c)$ plane can be divided into regions which indicate where both thermal and viscous instability occur.

When an experimentally determined $\epsilon - v_c$ relationship becomes available, Fig. 7 may be used to map out the region of instability. For the purpose of illustration, we construct four hypothetical experimental results in Fig. 7. Curve (a) represents thermal instability over the entire range of ϵ; curve (b) represents viscous instability over a certain range of ϵ and marginal thermal and viscous instability otherwise; and curves (c) and (d) represent viscous instability over a certain range of ϵ and stability for $\epsilon < \epsilon_c$ or ϵ_d, respectively. Curve (d) corresponds to the power-law $\epsilon - v_c$ relation assumed by Ward (1981), with $\alpha = 10$. When these results are analysed together with the $\epsilon - \tau$ relationship (Eq. 37), each value of ϵ corresponds to an optical depth. Physically, curve (a) would cause a ring to evolve into a torus or a thin sheet on dynamical time scales. Curve (b) would cause a ring system to break into many ringlets separated by gaps with arbitrarily small τ. Curves (c) or (d) would cause a ring system to break into ringlets separated by gaps with finite optical depth. Voyager's data on Saturn's B Ring indicate that the ringlets are separated by gaps with moderate optical depth (chapter by Cuzzi et al.). If the ringlet structure is caused by a viscous instability, these data suggest

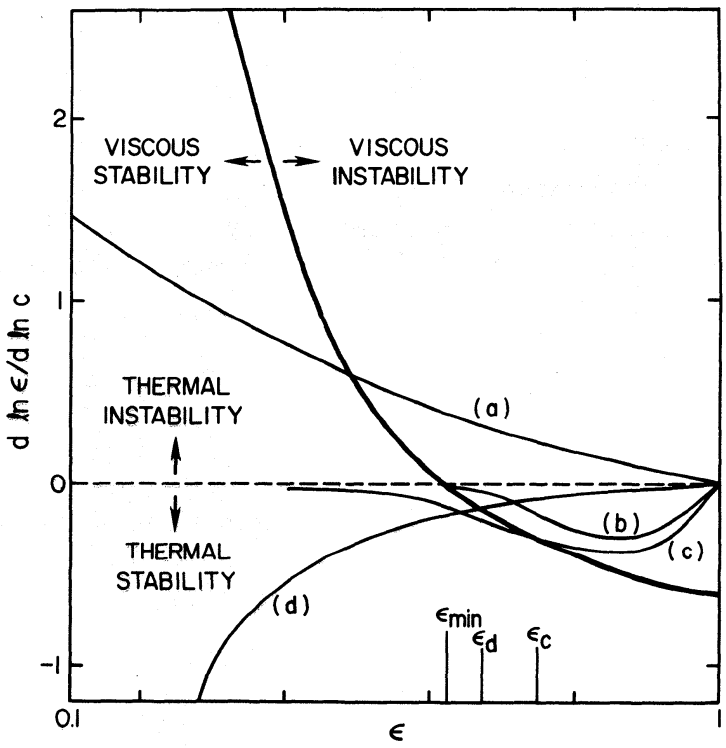

Fig. 7. The $\epsilon - c$ relation ($\epsilon - v_c$ relation) plotted as a function of ϵ. The critical line for viscous instability, defined by Eq. (88) is given by the heavy solid curve. Hypothetical $\epsilon - c$ relations, as explained in the text, are plotted as curves a, b, c, and d. Equilibrium solutions are allowed only to the right of ϵ_{min} and below the dashed line.

that the intrinsic properties of the ring particles may indeed be similar to those portrayed in curve (c).

Both preliminary experimental data (Bridges et al. 1984) and theoretical impact models (chapter by Borderies, et al.) give results similar to curve (c). However, both of these results are based on ring particles that are modeled as solid ice spheres. It is entirely possible that some degree of fragmentation or aggregation of ring particles actually occurs during collisions. In that case substantial regoliths may be built up on the larger ring particles which could greatly alter their restitution coefficient (see chapter by Weidenschilling et al.). For particles which are not perfect spheres, the restitution coefficient may depend on the orientation of the collision and particle spin as well as on the impact velocity. Although these effects may be important, they are much too complex to be considered here.

2. Kinetic Approach. In the above fluid-dynamical analyses, only the trace of the velocity-dispersion ellipsoid is analyzed. In reality, we have assumed $T_{r\theta}/\mathrm{Tr}\ \mathbf{T}$ only depends on τ as expressed in Eq. (52). This assumption may be relaxed when the stability analysis is carried out with the kinetic

approach. In this case, medium-wavelength perturbations must be introduced to $T_{rr}, T_{r\theta}, T_{\theta\theta}$, and T_{zz} so that we must solve for the linearized mass diffusion equation and all four components of the second-order moment equation. Such a computation may be carried out numerically along the same lines that Goldreich and Tremaine (1978) used to deduce the transport coefficient (see Sec. II.B.3). Alternatively, the approximate analytic results obtained by Hämeen-Anttila (1978) (see also Sec. II.B.3) may be used to make somewhat further analytical advances. Applying the perturbation into Eqs. (38) yields five linearlized equations. Preliminary eigenvalue results indicate that the condition for viscous instability is not changed. However, the analysis for thermal instability becomes much more complex, and it may be necessary to solve it numerically. The above results clearly indicate the advantages and the limitation of the fluid-dynamical approach. While it does simplify stability analyses considerably, it must be based on certain assumptions.

C. Thermal and Viscous Stability at Very Short Wavelength

The viscous instability criterion deduced in Sec. IV.B (i.e., Eq. 88) does not contain any wavelength dependence. Literal interpretation of this result implies that when the ring becomes unstable, it may be divided into ringlets with arbitrarily small width. If this is the case, the validity of the hydrodynamic approximation, on which the entire rigorous analyses are based, becomes questionable. However, at very small wavelength several physical effects become important. For example, the pressure gradient effect, due to large gradients in τ and c, may cause the flow to depart significantly from Keplerian rotation and to induce a large radial velocity which would enhance the previously negligible advective transport processes. In addition, the conductive process also becomes important. Thus, some basic assumptions in standard analyses of ring structure, such as the stationary and Keplerian nature of Ω and the magnitude of u_r, must be relaxed. These effects can only be taken into account if short-wavelength perturbations are also introduced to Ωr and u_r and their evolution is analyzed with the momentum equation, in the fluid approximation, or the first-moment equation, in the kinetic approach. In the fluid case, four equations, i.e., Eqs. (49), (50a), (50b), and (53) must be solved simultaneously. Preliminary eigenvalue analysis of the linearized equations indicate no simple analytical criteria for thermal or viscous instability.

Although the fluid approximation for instability analysis is very attractive, due to its simplicity, there are several limitations to its applicability to planetary rings. First, as we have stated in Sec. IV.B, it is based on the assumption that the transport coefficients, such as the viscosity, are not changed by the perturbations. Second, a functional form for the conductive coefficient has to be introduced. Third, it is difficult to find unambiguous correspondence between certain terms in the fluid dynamical transport equations and others in the kinetic moment equations. These problems may be obviated with the kinetic treatment. In this case, seven linearized perturbation

equations must be solved simultaneously. Besides the difficulties associated with obtaining and interpreting the eigenvalue solutions of a 7×7 matrix, the truncation of the third-order pressure tensor becomes problematic. Obviously, we cannot proceed on this topic without considerable additional complications. Therefore, we leave discussion of this aspect of stability analyses to further progress in the field.

V. VISCOUS STABILITY AT LARGE AND SMALL OPTICAL DEPTH

One of the most important applications of the stability analyses presented in Sec. IV is to provide a scenario for the origin of the ringlets. If the ringlet structure is indeed caused by the diffusion instability, it is relevant to discuss the evolution of the ring after the onset of the instability. In the preliminary discussion in Sec. IV.A we argued that, when an infinitesimal perturbation is imposed on a ring system with moderate τ, ring particles continually drift from regions with a deficit surface density into regions with an enhanced surface density so that the contrast between the ringlets and the gaps increases with time. However, Voyager data on Saturn's B Ring indicate that variations in optical depth between the ringlets and the gaps are relatively moderate and that transitions between those regions can be resolved. These data suggest that if the ringlet structure is indeed due to a viscous instability, there must be stabilizing effects at both high and low optical depth limits. There are several stabilizing mechanisms:

1. At sufficiently large τ, c becomes so small that gravitational attraction between particles may become important;
2. Also at large τ, the mean free path of the particles cannot be reduced below the size (R_p) of a typical particle, so that there is a lower limit to the magnitude of ν.
3. At small τ, the form of the $\epsilon - v_c$ relation may lead to a viscous stress that increases with c for τ less than some critical value (see Sec. IV.B.1), in which case the disk is stabilized.

In this section we first discuss stabilizing effects at large τ and then at small τ.

A. Self-gravitating Effects at Large τ

Depending on the values of c and σ, gravitational attraction between ring particles can produce at least three significant effects:

1. It induces gravitational scattering through which a minimum c may be maintained (Cuzzi et al. 1979; Ward and Harris 1983);

2. It increases the frequency of mid-plane crossings as a result of additional gravitational pull towards the mid-plane of the ring (Salo and Lukkari 1982);
3. It may lead to collective gravitational instability.

1. Gravitational Scattering, Thermal Stability and Minimum c. Gravitational scattering between ring particles becomes important when their relative velocity $g = \max(\sqrt{2}c, \Omega R_p)$ is less than the surface escape velocity from a particle, $V_{esc} = (8\pi G\rho/3)^{\frac{1}{2}} R_p$. For ring particles made of ice (density 1 g cm^{-3}), gravitational scattering between ring particles becomes important if g is sufficiently small that the ring's thickness is less than

$$H_{esc} \simeq V_{esc}/\Omega = 1.8\,(r/R_s)^{\frac{3}{2}} R_p \tag{89}$$

where R_s is the radius of Saturn. At the inner edge of Saturn's A Ring where $r = 2.0\,R_s$, and for a particle of 5 m radius, $H_{esc}/\sqrt{2} = 18$ m. Thus gravitational scattering between particles only plays an important role if the scale height of the ring is less than a few particle radii (Goldreich and Tremaine 1982). If there is a broad distribution of particle sizes, however, gravitational scattering more strongly influences the smaller particles because they can pass closer to a larger particle without suffering a collision (see Sec. VI.C.).

Gravitational scattering is a purely elastic process ($\epsilon = 1$) which merely stirs random motion without causing dissipation. The increase in velocity dispersion caused by a scattering event between two particles with separation $r_{12} = |\mathbf{r}_1 - \mathbf{r}_2|$ is on the order of $\Delta c \sim Gm/r_{12}c$. This mechanism will tend to increase c until $(\Delta c)^2$ is reduced to the point where the total energy input rate due to both gravitational scattering and direct collisions balances the energy dissipation rate due to the inelasticity of collisions. The inverse relation between Δc and c for gravitational scattering will always allow the system to adjust to a thermal equilibrium state provided there is a finite level of energy dissipation which does not rapidly decrease with increasing c.

Thus, gravitational scattering may effectively maintain a velocity dispersion of the same order as the surface escape velocity from the particle size which represents most of the mass of the rings. Further discussion of this process may be found in Ward's chapter. This lower limit on c implies that the $\epsilon - \tau$ relationships derived in Sec. I (Eq. 13) and Sec. II (Eq. 43) must be somewhat modified to take into account the fact that only a fraction of the collisions are dissipational. Similarly, the criteria for thermal and diffusion instability (Eqs. 86 and 88) must also be modified.

Gravitational scattering plays a predominant role in the context of the protoplanetary accretion disk (see Ward's chapter). However, its contribution is of marginal importance in typical planetary rings because the scattering cross section, which is limited to H_{esc}^2 by the thin disk geometry, never greatly exceeds the physical cross section of a typical ring particle. In addition,

typical planetary rings usually lie within two planetary radii. At this distance, the central planet can exert a gravitational influence on the surface of a typical ring particle that has a strength comparable to that due to the ring particle itself unless the internal density of the ring particle considerably exceeds that of the planet. Thus, the tidal radius of a typical particle does not extend much beyond its surface. In this case, the gravitational interaction between neighboring particles tends to occur inside the Roche radius of the central planet itself. This planetary tidal influence tends to decrease the efficiency of gravitational scattering between particles. Mathematically, the planetary tidal influence may be analyzed numerically by integration of the 3-body orbits (see chapter by Weidenschilling et al.).

Although gravitational scattering may only play a limited role in the dynamics of a planetary ring, it can stabilize the viscous instability at large τ. In particular, a lower limit on c implies a lower limit on ν. If a ring is viscously unstable, c would decrease as τ increased in a ringlet. Eventually, τ would become sufficiently large and c sufficiently small so that gravitational scattering would become important. Then ν would no longer decrease as τ increased and the ring would become stabilized. Finally, it should be pointed out that at large τ, the interparticle spacing may become so small that the gravitational potential energy is comparable to the kinetic energy of relative motion. In this case, the kinetic theory described in Sec. II.B breaks down and a more complicated approach analogous to the theory of liquids must be applied.

2. Enhancement in Plane-crossing Frequency. The increase in the frequency of passages through the mid-plane of the ring results in an increased collisional frequency and thus an increased shear stress at large τ (Salo and Lukkari 1982). The stability analyses in Sec. IV.A indicate that a ring is stabilized against viscous diffusion if viscous stress increases with τ.

In the limit of small orbital inclination, the out-of-plane motion of a ring particle can be described by

$$\ddot{z} = -\Omega^2 z + f_z \tag{90}$$

where f_z is the force due to self gravity of the ring which may be obtained from Gauss's law:

$$f_z = -2\pi G\sigma(z) \ . \tag{91}$$

The quantity $\sigma(z) = m\int_{-z}^{z} N(z')dz'$ is that fraction of the ring's surface density contained between z and $-z$. Let us assume that $N(z)$ has the Gaussian form of Eq. (29), except that $\overline{z^2}$ is now depressed below its unperturbed value, $\overline{z_0^2} = T_{zz}/\Omega^2$, by the force f_z. Equation (91) may be expanded for small z such that

$$f_z = -2\pi GmN(0)\int_{-z}^{z}\left[1 - z'^2/(2\overline{z^2}) + \ldots\right]dz'$$
$$= -2\sqrt{2\pi}G\sigma\left[z/(\overline{z^2})^{-\frac{1}{2}} - \left(z^3/6\right)\left(\overline{z^2}\right)^{-\frac{3}{2}} + \ldots\right]. \quad (92)$$

Keeping only terms linear in z, the equation of motion becomes

$$\ddot{z} = -\Omega_*^2 z \text{ where } \Omega_*^2 = \Omega^2\left[1 + 2\left(\frac{2\pi}{\overline{z^2}}\right)^{\frac{1}{2}}\frac{G\sigma}{\Omega^2}\right]. \quad (93)$$

The above result indicates that the self-gravity of the ring effectively increases the frequency of vertical oscillations across the mid-plane of the ring by a factor Ω_*/Ω. The reduced scale height $\overline{z^2}$ is given by the equation

$$\overline{z^2} + 2\sqrt{2\pi}G\sigma\left(\overline{z^2}\right)^{\frac{1}{2}}/\Omega^2 - T_{zz}/\Omega = 0 \quad (94)$$

which results from setting T_{zz}/Ω_*^2 equal to $\overline{z^2}$. Solving for $\overline{z^2}$ one finds

$$\Omega_*/\Omega = \left[(1+\Delta^2)^{\frac{1}{2}} + \Delta\right] \text{ where } \Delta = \left(\frac{2\pi}{T_{zz}}\right)^{\frac{1}{2}}\frac{G\sigma}{\Omega}. \quad (95)$$

Both the increase in the frequency of oscillation across the mid-plane and the decrease in the scale height induce increases in the collisional frequency and shear viscosity. One may expect that this effect increases the collision frequency by a factor of 2 at most. The net result is to enhance the stabilizing effect of finite particle size (see Sec. V.B below) at large optical depth (Salo and Lukkari 1982).

3. Gravitational Instability. Toomre (1964) has shown that, in the context of galactic disks, a collisionless particle ring may become gravitationally unstable against axisymmetric perturbations if the radial component of the dispersion velocity ellipsoid drops below the value

$$(T_{rr})_{\min}^{\frac{1}{2}} = 3.36\,G\sigma/\Omega. \quad (96)$$

Since internal energy associated with dispersive motion cannot be dissipated in a collisionless stellar system, such as a spiral galaxy, this gravitational instability acts to virialize the particles in the sense that it provides a stirring mechanism which effectively prevents the velocity dispersion from falling below $(T_{rr})_{\min}^{\frac{1}{2}}$. In a gravitationally unstable planetary ring, internal energy may still be lost through dissipative collisions at a rate which may reduce somewhat the critical minimum dispersion velocity (Goldreich and Tremaine 1982). We have already stated that typical ring particles have physical sizes

comparable to their tidal radii. Nevertheless, gravitational instability can occur since it is caused by a collective interaction of a large number of particles. The axisymmetric instability leads to a ring-like density enhancement which at close range acts on nearby particles with an attractive gravitational force that decreases as the inverse of the distance from the ring rather than the inverse square.

Harris and Ward (1983) have suggested that the transient collective motion induced by the gravitational instabilities may result in an effective kinematic viscosity ν_e which may be defined in an expression analogous to Eq. (12):

$$\nu_e (3\Omega/2)^2 = (1-\epsilon^2)\,\omega_c\, c_{\min}^2 . \tag{97}$$

If the minimum velocity dispersion $c_{\min}$, has the approximate form of Eq. (96), the effective kinematic viscosity would be

$$\nu_e = K(1-\epsilon^2) G^2 \sigma_0^2 \tau^3/\Omega^3 \tag{98}$$

where $\sigma_0 = \sigma/\tau$ is the surface density at unit optical depth and K is a constant ~ 0.1 to 10. With such an effective viscosity, the viscous stress increases with τ^4 such that the ring is stable against viscous diffusion. Since gravitational instability can only occur for large τ, the above result may be interpreted as a stabilizing effect which acts to prevent τ from increasing beyond a certain level.

B. Effect of Finite Size of Particles at Large τ

The finite size of the particles induces and maintains a residual relative velocity, ΩR_p, that can not be damped out regardless of the efficiency of the collisional dissipation (Brahic 1977). This residual relative velocity, which is comparable to the difference in Keplerian velocity between particles with orbits separated by $2R_p$, provides a lower limit to the magnitude of the kinematic viscosity (Goldreich and Tremaine 1982):

$$\nu_{\min} \simeq \omega_c R_p^2 \simeq \Omega R_p^2 \tau . \tag{99}$$

This minimum viscosity exceeds ν_e (Eq. 98) for particles with size larger than $R_{p,\min} \simeq KG\sigma/\Omega^2$. In Saturn's rings, for example, $\sigma \approx 50$ g cm^{-2} and $\Omega \approx 2 \times 10^{-4}$ s^{-1} so that $R_{p,\min}$ is about K m. Unless K is much larger than unity, direct physical collisions among particles larger than meter size can be more efficient than gravitational instability in preventing c from decreasing below a certain critical value at large τ.

The above qualitative deductions may be substantiated with a more rigorous mathematical analysis. For simplicity, such a calculation may be based on the assumption that the ring is composed of uniform hard spheres with a

collision law as prescribed by Eq. (10). The second velocity moment of the collisional integral (Eq. 21) may be written in the form (Trulsen 1971)

$$\left(\frac{\partial p_{ij}}{\partial t}\right)_c = 2R_p^2 \iiint \left[\mathbf{v}_{1a}\,\mathbf{v}_{1a} + \mathbf{v}_{2a}\,\mathbf{v}_{2a} - \mathbf{v}_{1b}\,\mathbf{v}_{1b} - \mathbf{v}_{2b}\,\mathbf{v}_{2b}\right] \times (\mathbf{g}\cdot\hat{\mathbf{k}}) f(\mathbf{v}_{1b}) f(\mathbf{v}_{2b})\, \mathrm{d}\hat{k}\, d^3 \mathrm{v}_{1b}\, d^3 \mathrm{v}_{2b} \tag{100}$$

where the post-collisional velocity is related to the pre-collisional velocity by

$$\mathrm{v}_{1,2,a} = \mathrm{v}_{1,2,b} \mp 0.5\,(1+\epsilon)\,(\mathbf{g}\cdot\hat{\mathbf{k}})\hat{\mathbf{k}}\ . \tag{101}$$

In the limit of vanishing velocity dispersion Eq. (100) becomes

$$\left(\frac{\partial p_{ij}}{\partial t}\right)_c = N^2 R_p^2\,(1+\epsilon)^2 \int (\mathbf{g}\cdot\hat{\mathbf{k}})^3 \hat{\mathbf{k}}\,\hat{\mathbf{k}}\,\mathrm{d}\,\hat{\mathbf{k}}\ . \tag{102}$$

The evaluation of the above integral depends on the direction of the relative velocity **g**.

Now consider a collision between two neighboring particles, which are originally on circular Keplerian orbits. It is mathematically convenient to analyze the collision in a rotating Cartesian coordinate system (r_1, θ_1, z_1) which is centered on particle 1 (see Fig. 8) and which corotates with the position vector of particle 1. Suppose that it is on a collision course with particle 2. Due to the difference in their positions in the ring, the direction as well as the magnitude of the orbital velocities, v_1 and v_2, of the two particles may differ (see Fig. 8). To first order in R_p/r, **g** may be expressed in the newly defined coordinates such that

$$\mathbf{g} = (-\mathrm{v}_2 \sin\delta,\ \mathrm{v}_2\cos\delta - \mathrm{v}_1,\ 0) \simeq [-\Omega r_2\delta,\ -\tfrac{1}{2}\Omega\,(r_2 - r_1),\ 0] \tag{103}$$

where δ is the angle between the position vectors of the colliding particles. The directional vector $\hat{\mathbf{k}}$, pointing to the center of particle 2, is

$$\hat{\mathbf{k}} = (\sin\psi\cos\phi,\ \cos\psi,\ \sin\psi\sin\phi) \tag{104}$$

where ψ is the angle between the θ_1-axis and $\hat{\mathbf{k}}$ and ϕ is the angle between the r_1 axis and the projection of $\hat{\mathbf{k}}$ onto the $r_1 - z_1$ plane. For finite values of ϕ, Eqs. (103) and (104) actually describes collisions between particles in circular orbits distributed in parallel planes a distance $z \neq 0$ above the mid-plane. Although such a situation is not possible in reality, the inclusion of such orbits provides

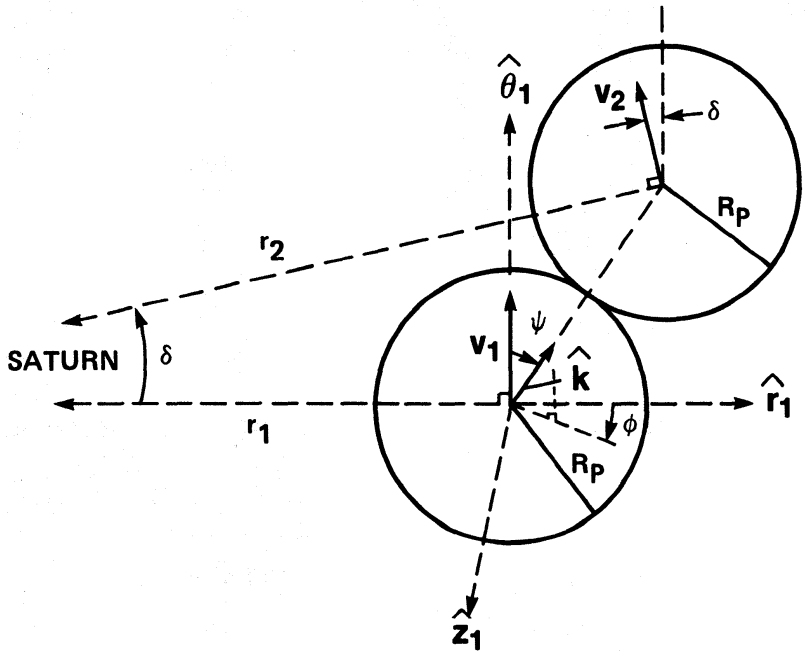

Fig. 8. Geometry of collisions between hard spheres in circular orbits of radius r_1 and r_2 with velocities $\mathbf{v}_1$ and $\mathbf{v}_2$.

a useful channel for interpolating between the two extreme physical situations of large velocity dispersion ($c >> \Omega R_p$) and strictly coplanar, concentric, circular orbits ($c = 0$) (Hämeen-Anttila 1982). In terms of this geometry,

$$\mathbf{g} = -\Omega R_p\,(2\cos\psi, \sin\psi\cos\phi, 0). \tag{105}$$

By substitution of Eqs. (104) and (105) into the integral in Eq. (102), $(\partial p_{ij}/\partial t)_c$ may be evaluated in the restricted range ($0 < \psi < \pi/2$ and $-\pi/2 < \phi < \pi/2$ for $r_1 < r_2$; $\pi/2 < \psi < \pi$ and $\pi/2 < \phi < 3\pi/2$ for $r_1 > r_2$). The result of the integration is

$$\left(\frac{\partial p_{ij}}{\partial t}\right)_c = \frac{8}{35}\,\frac{N\tau(1+\epsilon)^2\Omega^3 R_p^3}{\pi(\pi\overline{z^2})^{\frac{1}{2}}}\begin{pmatrix} 4 & 9\pi/8 & 0 \\ 9\pi/8 & 4 & 0 \\ 0 & 0 & 1 \end{pmatrix}. \tag{106}$$

This expression is entirely analogous to a similar expression obtained by Hämeen-Anttila (1982).

In reality, collisions due to overlapping circular orbits always induce a true velocity dispersion that is of random nature. This effect can be incorporated into the evaluation of $(\partial p_{ij}/\partial t)_c$. Instead of simply adding the two contributions (Eq. 27) and (Eq. 106) for $(\partial p_{ij}/\partial t)_c$, Hämeen-Anttila (1982) suggests an interpolation formula of the form

$$\left(\frac{\partial p_{ij}}{\partial t}\right)_c = \omega_0^* \left\{ \frac{(1+\epsilon)}{18}\left[(1+\epsilon)\,\mathbf{Tr}\,\mathbf{p}\,\delta_{ij} - 3(3-\epsilon)p_{ij}\right] + \frac{(1+\epsilon)^2}{35} N(\Omega R_p)^2 \begin{pmatrix} 4 & 9\pi/8 & 0 \\ 9\pi/8 & 4 & 0 \\ 0 & 0 & 1 \end{pmatrix} \right\} \tag{107}$$

where

$$\omega_0^* = \frac{8\tau\Omega}{\pi}\left[\frac{\mathrm{Tr}\mathbf{T} + (3/\pi)(\Omega R_p)^2}{3\Omega^2 \overline{z^2}}\right]^{\frac{1}{2}} \tag{108}$$

is the collision frequency. The advantage of the above expression is that it is approximately valid for both large and small velocity dispersion. If a planetary ring is in an energy equilibrium, the energy transport Eq. (36) reduces to

$$T_{r\theta}(3\Omega/2) = \omega_0^* \left[\frac{1-\epsilon^2}{6}\mathrm{Tr}\mathbf{T} - \frac{9}{70}(1+\epsilon)^2(\Omega R_p)^2\right]. \tag{109}$$

This result differs from Eq. (40) since it contains an extra energy source term due to the finite size of the particles.

Following the same procedure used in Sec. II.B.4, we can deduce a generalized $\epsilon-\tau$ relationship such that

$$\tau = \frac{\pi\omega_0^*}{8\Omega}\left(\frac{1+\epsilon}{3-\epsilon}\right)^{\frac{1}{2}}\left[\frac{1+(18/35)(R_p\,\Omega)^2/\mathrm{Tr}\mathbf{T}}{1+(3/\pi)(R_p\,\Omega)^2/\mathrm{Tr}\mathbf{T}}\right]^{\frac{1}{2}}\left[(1+\Delta^2)^{\frac{1}{2}}-\Delta\right] \tag{110}$$

where

$$\Delta = \frac{G\sigma}{\Omega}\left[\frac{6\pi(3-\epsilon)}{(1+\epsilon)\left[\mathrm{Tr}\mathbf{T} + (18/35)(\Omega R_p)^2\right]}\right]^{\frac{1}{2}} \tag{111}$$

and

$$\frac{\omega_0^*}{\Omega} = \frac{-B + \sqrt{B^2 - 4AC}}{2A} \tag{112}$$

where

$$A = \left[\frac{(1+\epsilon^2)}{9}\mathrm{Tr}\mathbf{T} - \frac{3}{35}(1+\epsilon)^2(\Omega R_p)^2\right]\frac{(1+\epsilon)^2(3-\epsilon)^2}{36} \tag{113a}$$

$$B = \frac{-3\pi}{560}(1+\epsilon)^3(3-\epsilon)(\Omega R_p)^2 \tag{113b}$$

$$C = -\frac{(19\epsilon - 13)(1+\epsilon)}{36}\,\mathrm{Tr}\mathbf{T} - \frac{18}{35}(1+\epsilon)^2(\Omega R_p)^2 . \qquad (113c)$$

Although the above expression reduces to the original $\epsilon-\tau$ relationship (see Eq. 43) in the limit of very small particle size, there are some fundamental differences between the above formula and our previous results. For example, the new expression depends explicitly on $\mathrm{Tr}\mathbf{T}$. Therefore, an $\epsilon-v_c$ relationship is needed to deduce a unique $\epsilon-\tau$ relationship. Moreover, there is an explicit dependence on ΩR_p. The factor depending on Δ accounts for the increased collision frequency due to the vertical component of self-gravity discussed in Sec. V.A.2. These additional terms all contribute to stabilization against viscous diffusion at large τ since they provide a lower limit for ν. Mathematically, once an $\epsilon-\tau$ relationship is established, the shear stress may be calculated as a function of τ from Eq. (109), using Eq. (112) for ω_δ^*. This procedure leads to stress curves qualitatively similar to those in Fig. 9. Unfortunately, detailed quantitative analyses cannot be carried out until an $\epsilon-v_c$ relationship is available.

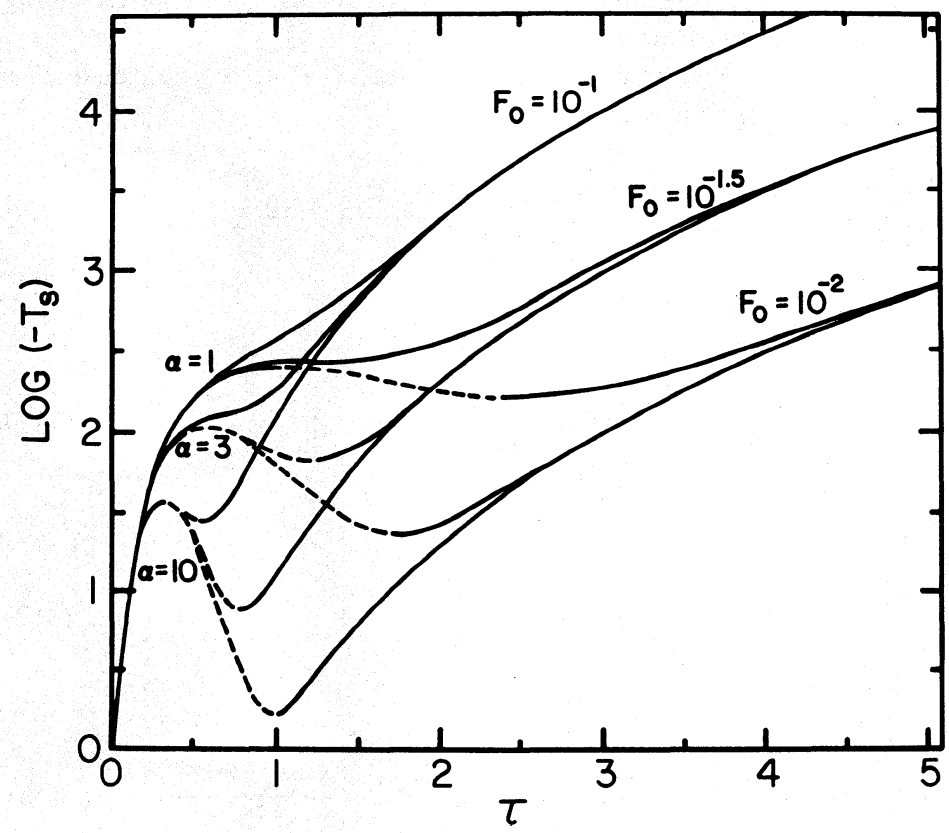

Fig. 9. The viscous torque $T_s = 2\pi r^3\,\sigma\nu\partial\Omega/\partial r$ plotted as a function of τ. Curves are parameterized by the value of α and F_0 as explained in the text (figure from Harris and Ward 1983).

C. Stabilizing Effect at Small τ

If a ring is thermally stable, c must decrease with τ. The condition for an energy equilibrium (Eq. 13) indicates that ϵ increases with τ. Thus, in a thermally stable ring low optical depth corresponds to large velocity dispersion. For relatively large dispersion velocities, gravitational scattering occurs less frequently than direct collision so that the self-gravitating effects discussed in Sec. V.A are negligibly small. Similarly, the finite size of the particles does not influence the dynamics of the ring except that it provides a cross section for direct physical impact. Consequently, stabilization against the viscous diffusion instability at small τ must occur because of the intrinsic collisional properties of the particles themselves. As we have discussed in Sec. V.B.1, an $\epsilon-v_c$ relationship similar to curve (c) in Fig. 7 can stabilize a ring at $\tau<\tau_c$.

D. Comparisons with Observations

In order to verify that the viscous diffusion instability scenario is a reasonable explanation for the origin of the ringlets, several observable parameters need to be deduced. Voyager's data contains a vast amount of information on the optical depth variation in the ringlet systems (chapter by Cuzzi et al.). If we combine the above results on the condition for viscous instability and the stabilizing effects at large and small τ, we can make a direct comparison between the theory and the Voyager data. The above discussion indicates that the stability criterion may depend sensitively on the $\epsilon-v_c$ relationship. However, due to the lack of an experimentally determined $\epsilon-v_c$ law, most of the previous work is based on *ad hoc* assumptions. For example, in order to obtain a $\nu-\tau$ relation valid for both large and small τ, Harris and Ward (1983) simply added Eq. (98) to the viscosity formula (52). Figure 9 shows the logarithm of the resultant viscous stress as a function of τ for various *ad hoc* $\epsilon-v_c$ laws parameterized by $\alpha = \mathrm{d}\ln c^2/\mathrm{d}\ln(1-\epsilon^2)$ and for various filling factors $F_0 = \Omega R_p/c_0$, where c_0 is the equilibrium velocity dispersion obtained from Eq. (12) in the limit of very small τ. The viscous stress typically exhibits a local minimum value at τ near unity. Once a viscous diffusion instability occurs, the local optical depth may grow until the ringlet is stabilized at the optical depth corresponding to this minimum stress value $S_{\min}$. The adjacent gaps would be stabilized at the smaller (but nonzero) τ where the viscous stress again attains the value $S_{\min}$. Thus, ringlet formation may induce a stress value considerably lower than that deduced for a uniform τ. The precise value of τ at which the ring is stabilized may eventually be determined once all of the stabilizing mechanisms discussed in this section are included in the theory and an $\epsilon-v_c$ law is available. However, an important further modification discussed in the next section may arise from the observed fact that there is a broad distribution of particle sizes.

VI. THE EFFECT OF A PARTICLE SIZE DISTRIBUTION

A. Implications of Observational Data

So far, the analyses have been limited to planetary rings with uniform particle size. We adopted this case to study first since it simplifies the mathematical procedures considerably. However, Voyager's radio occultation measurement of Saturn's A Ring (Marouf et al. 1983; chapter by Cuzzi et al.) can be approximated by a power-law distribution in the number density $N(R_p)$ of the form

$$dN(R_p) = \begin{cases} A R_p^{-q} dR_p, & \text{for } 1 \text{ cm} < R_p < 5 \text{ m} \\ 0, & \text{for } R_p < 1 \text{ cm or } R_p > 5 \text{ m} \end{cases} \tag{114}$$

where $2.8 < q < 3.4$. A similar power law is observed in the asteroid belt (Anders 1965) and may be generally representative of collisional particle disks (chapter by Weidenschilling et al.). For simplicity, we adopt $q = 3$ for the discussion below.

Particles with radii between $R_{p,1}$ and $R_{p,2}$ contribute an optical depth

$$\tau_{12} = \int_{R_{p,1}}^{R_{p,2}} \pi R_p^2 dN(R_p) = \tau \frac{\log(R_{p,2}/R_{p,1})}{\log(500)} \tag{115}$$

where τ is the total optical depth due to all the particles. This result implies that the observed optical depth represents comparable contributions from particles in each size range if q ~ 3. However, particles with $R_{p,1} < R_p < R_{p,2}$ contain a fractional mass

$$\Delta M = \int_{R_{p,1}}^{R_{p,2}} \frac{4}{3} \rho \pi R_p^3 dN(R_p) = \frac{4\rho\tau(R_{p,2} - R_{p,1})}{3 \log(500)} \tag{116}$$

which implies that 80% of the total ring mass is contained in particles with $R_p > 1$ m.

It is also of interest to estimate the mean spacing d between particles within a given size range, a quantity which may be deduced once the scale height of the ring is determined from the condition for an energy equilibrium. Such a calculation requires the generalization of the second-order moment Eqs. (38) consistent with this size distribution along with an experimentally determined $\epsilon - v_c$ law. These analyses remain to be carried out. Nonetheless, an order of magnitude value for d may be estimated in a qualitative manner. For example, suppose that the scale height for all particles is comparable to

the size of the largest particles and τ is on the order of unity. In this case, the largest meter-sized particles in the distribution (Eq. 114) would be separated by a distance comparable to their own diameters, while the smallest cm-sized particles would be separated by ten times their own diameters. The implications are two fold. First, successive gravitational encounters with the largest m-sized particles, by either small or large particles, may not be well-separated events. Thus, mathematical analyses based on simple 3-body gravitational scattering (see Sec. V.A.1) may be inadequate. Second, the large m-sized particles have more frequent encounters with smaller cm-sized particles than with themselves. The collisional frequency $\omega_{i\to j}$ between particles with different sizes, say $R_{p,i}$ and $R_{p,j}$ can be estimated from

$$\omega_{i\to j} = \Omega\tau_j (1 + R_{p,i}/R_{p,j})^2 . \qquad (117)$$

The inferences from the above equation are: (1) a cm-sized particle collides on the average with four other cm-sized particles before colliding with a m-sized particle, and (2) a m-sized particle collides with several thousand cm-sized particles between collisions with another m-sized particle.

Although $\omega_{2\to 1}/\Omega >> 1$ for $R_{p,1} << R_{p,2}$, the presence of small cm-sized particles hardly influences the viscous evolution of the large m-sized particles since most of the ring's mass is contained in the large particles. Therefore, the stability analyses based on uniform particle size are applicable to the large m-sized particles. In contrast, small cm-sized particles collide as frequently with much larger particles as with themselves. Thus, the viscous evolution of the small particles is strongly coupled to the number density and the velocity dispersion of particles of all sizes. Consequently, viscous instability for the small cm-sized particles may be distinctly different from that in the case of uniform particle size.

B. Collisional Evolution of the Small Particles in a Bimodal Size Distribution.

1. Qualitative Analysis. For simplicity, the evolution of a ring with nonuniform particle sizes may be first illustrated with a simple qualitative analysis of a bimodal size distribution where $m_1 << m_2$ and τ_1/τ_2 is a constant of order unity. According to the argument presented in Sec. VI.A, the dynamics of the large particles are not influenced by the motion of the small particles. Since small particles collide often with the large particles, their evolution is strongly influenced by the kinetic state of the large particles. For example, if the large particles have zero dispersion velocity, then their main effect will simply be to limit the mean free path of the small particles. An effective mean free path may be obtained from Eq. (6) if we replace τ with $(\omega_{1\to 1} + \omega_{1\to 2})/\Omega$. The corresponding effective viscosity acting on the small particles has the form

$$\nu_1 = \frac{c_1^2}{\Omega} \frac{(\tau_1 + q\,\tau_2)}{1 + (\tau_1 + q\,\tau_2)^2} \tag{118}$$

where c_1 is the dispersion velocity of the small particles and $q \sim 2$ for $R_1 << R_2$ (Stewart 1984).

In the case that the large particles have a finite velocity dispersion, the mean free path of the small particles will be somewhat larger than the above estimate. The velocity change of particle 1 resulting from a collision with particle 2 is

$$\mathbf{v}_{1a} - \mathbf{v}_{1b} = -\frac{m_2\,(1+\epsilon)}{m_1 + m_2} (\mathbf{v}_{1b} - \mathbf{v}_{2b}) \cdot \hat{\mathbf{k}}\,\hat{\mathbf{k}} \ . \tag{119}$$

Since the velocity components of different particle sizes are uncorrelated, Eq. (119) requires the mean square velocity change of particle 1 due to non-zero dispersion velocity of the large particles c_2 to be proportional to c_2^2. In the limit of large collision frequency the additional contribution to the mean free path of the small particles is just $c_2/(\omega_{1\to 1} + \omega_{1\to 2})$. The total ν_1 in this limit therefore becomes

$$\nu_1 = \frac{c_1^2 + c_2^2}{\Omega\,(\tau_1 + q\,\tau_2)} \quad \text{for } \tau_1 \text{ and } \tau_2 >> 1 \ . \tag{120}$$

In the low-τ limit the calculation of the mean free path is complicated by the epicyclic motion of the particles. Consider the approximate equation of motion of particle 1 in the reference frame of its circular orbital motion:

$$\frac{\partial \mathbf{v}_1}{\partial t} + 2\mathbf{v}_1 \times \hat{\mathbf{z}}\,\Omega = -\omega_{1\to 1}\,\mathbf{v}_1 - \omega_{1\to 2}\,(\mathbf{v}_1 - \mathbf{v}_2) \ . \tag{121}$$

The right-hand side of the above equation estimates the time-averaged change in particle 1's velocity caused by infrequent collisions with particles 1 and 2. For $\omega_{1\to 1}$, $\omega_{1\to 2} << \Omega$ this equation may be solved with a series expansion $\mathbf{v}_1 = \mathbf{v}_1^0 + \mathbf{v}_1^1 + \ldots$ where $\mathbf{v}_1^0$ satisfies the collisionless approximation to Eq. (121).

$$\frac{\partial \mathbf{v}_1^0}{\partial t} + 2\mathbf{v}_1^0 \times \hat{\mathbf{z}}\,\Omega = 0 \ . \tag{122}$$

The small collision-induced average perturbation $\mathbf{v}_1^1$ is given by

$$2\mathbf{v}_1^1 \times \hat{\mathbf{z}}\,\Omega = -(\omega_{1\to 1} + \omega_{1\to 2})\,\mathbf{v}_1^0 + \omega_{1\to 2}\,\mathbf{v}_2^0 \ . \tag{123}$$

$\partial \mathbf{v}_1^1/\partial t$ does not appear in the above equation because $\mathbf{v}_1^1$ is the average change in $\mathbf{v}_1$ after many orbital periods. This relation indicates how small perturbations from the collisionless motion are of order ω_c/Ω times the relative velocity of the colliding bodies. Since $\mathbf{v}_1^0$ and $\mathbf{v}_2^0$ are uncorrelated, the resultant change in the mean square velocity of the small particles has just two contributions, $(\omega_{1\to 1} + \omega_{1\to 2})^2 c_1^2/\Omega^2$ and $\omega_{1\to 2}^2 c_2^2/\Omega^2$. The first of these contributions tends to decrease the velocity dispersion of the small particles and thereby decrease the radial mean free path. Thus, if $c_2 = 0$, the resultant shear viscosity for infrequent collisions is

$$\nu_1 = (\omega_{1\to 1} + \omega_{1\to 2}) \frac{[c_1^2 - c_1^2 (\omega_{1\to 1} + \omega_{1\to 2})^2/\Omega^2]}{\Omega^2}$$

$$\approx \frac{c_1^2}{\Omega}\left[\tau_1 + q\tau_2 - (\tau_1 + q\tau_2)^3\right] . \tag{124}$$

Note that Eq. (124) is just the low-τ expansion of Eq. (118). The second contribution to the small particles' velocity dispersion, $\omega_{1\to 2}^2 c_2^2/\Omega^2$, adds to c_1^2 because a finite c_2 can increase the post-collisional velocity and hence the mean free path of the small particles. The generalization to Eq. (124) is thus

$$\nu_1 = (\omega_{1\to 1} + \omega_{1\to 2})\,[c_1^2 - c_1^2 (\omega_{1\to 1} + \omega_{1\to 2})^2/\Omega^2 + c_2^2\,\omega_{1\to 2}^2/\Omega^2]/\Omega^2$$

$$\simeq \frac{1}{\Omega}\left\{(\tau_1 + q\tau_2)\left[1-(\tau_1 + q\tau_2)^2\right] c_1^2 + (\tau_1 + q\tau_2)\,(q\tau_2)^2\, c_2^2\right\} \tag{125}$$

for τ_1 and $\tau_2 << 1$.

The more rigorous calculation presented in the following section (VI.B.2) suggests a rough interpolation between Eqs. (120) and (125) of the form

$$\nu_1 \approx \frac{(\tau_1 + q\,\tau_2)\,[c_1^2 + q^2\,\tau_2^2\,c_2^2/(1 + q^2\,\tau_2^2)]}{\Omega[1 + (\tau_1 + q\,\tau_2)^2]} \tag{126}$$

The energy of random motion of the small particles, $\frac{1}{2}c_1^2$, increases at the rate $(9/4)\Omega^2\nu_1$ due to the above shear viscosity. In addition, the large particles transfer some of their energy of random motion to the small particles at the rate

$$\dot{E}_{\rm tr} \simeq \omega_{1\to 2}\left(c_2^2 - \frac{m_1}{m_2} c_1^2\right) . \tag{127}$$

This tendency toward energy equipartition would occur even in the absence of the systematic shear of the mean orbital motion. Because of the inelasticity of the collisions, however, the energy transfer rate is modified from that given in Eq. (127). The kinetic theory described below yields an actual energy transfer rate of the form

$$\dot{E}_{\rm tr} = \frac{\omega_{1\to 2} m_2}{3(m_1+m_2)} (1+\epsilon) \left[\frac{m_2(1+\epsilon)(c_1^2+c_2^2)}{m_1+m_2} - 2c_1^2 \right] . \tag{128}$$

This equation would reduce to the form of Eq. (127) in the perfectly elastic limit, $\epsilon = 1$. The energy balance equation for the small particles is now

$$\frac{9}{4} \Omega^2 \nu_1 + \dot{E}_{\rm tr} = (1-\epsilon^2) \omega_{1\to 1} c_1^2 \tag{129}$$

where ν_1 and $E_{\rm tr}$ are given by Eqs. (126) and (128), respectively. A solution for the steady-state c_1 can be obtained if Eq. (129) is supplemented by the energy balance equation for the large particles. If we neglect the effect of the small particles on c_2, the equation for a single particle size applies:

$$\frac{9}{4} \Omega^2 \nu_2 = (1-\epsilon^2) \omega_{2\to 2} c_2^2$$

$$\nu_2 = \frac{c_2^2 \tau_2}{\Omega (1+\tau_2^2)} . \tag{130}$$

Equations (129) and (130) may be used to find c_1^2 as a function of τ_1 and τ_2. It should be noted that the quantity ϵ, which appears in Eq. (128), should be evaluated at $v_c = (c_1^2 + c_2^2)^{\frac{1}{2}}$; however, in Eqs. (129) and (130) ϵ should be evaluated at $v_c = \sqrt{2}\, c_1$ and $\sqrt{2}\, c_2$, respectively. In general, one will derive a steady-state $m_1 c_1^2 / m_2 c_2^2 << 1$ because ν_1 results in nonequipartition. Substituting the steady-state value of c_1^2 back into Eq. (126), one obtains a shear stress acting on the small particles proportional to $\tau_1 \nu_1$.

We find that the effect of large particles on small particles depends sensitively on the kinetic state of the large particles and the ratio τ_1/τ_2. In the case $c_2^2 < c_{cr}^2$, where c_{cr}^2 is some critical velocity between $(m_1/m_2)\, c_1^2$ and c_1^2, large particles merely reduce the mean free path which causes the maximum viscous stress, acting on the small particles, to attain a smaller value and to occur at a smaller $\tau = \tau_1 + \tau_2$. According to arguments in Sec. IV.C, a ring may be stable against viscous diffusion at sufficiently small τ if the $\epsilon - v_c$ law for the ring particles resembles that of curve (c) in Fig. 7. The above results suggest it is possible for the small particles to become viscously unstable even when the optical depth for each population may be smaller than the critical

value for instability in the case of a single particle size. This selective instability would tend to generate ringlets and gaps of small particles against a uniform background of large particles. As the density-enhanced region of the small particles grows, the effect of the large particles would diminish. However, the density enhancement in the small particles may continue owing to viscous instability among the small particles themselves. In the small-particle gaps, the large particles dominate and eventually stabilize the evolution of the small particles.

In the case $c_2^2 > c_{cr}^2$, collisions with large particles increase the velocity dispersion of the small particles more effectively than they limit the small particles' mean free path. The resultant viscous stress, therefore, increases with τ_2/τ_1. Thus, the large particles induce a stabilizing effect against viscous diffusion among the small particles. In this case, provided $\tau_1/\tau_2 \approx 1$, the small particles can only become viscously unstable when the large particles are also unstable.

Since the kinetic properties of the large particles are not affected by the small particles, c_2 may be deduced in terms of τ_2 from the energy equilibrium condition (Eq. 130) and $\epsilon - v_c$ law. Hence, there is a unique solution for a given value of τ_2. Furthermore, when an $\epsilon - v_c$ law is available, the evolution of viscous instability may be deduced for the two populations.

2. *Procedures for Rigorous Analysis*. The heuristic discussion in the preceding section may be verified with a rigorous analysis. We generalize the kinetic theory approach for hard-sphere collisions as presented in Sec. II.B.2. Let p_{ij} and P_{ij} be the pressure tensors associated with the probability densities $f(m_1, r_1, v_1, t)$ and $F(m_2, r_2, v_2, t)$. For the same reasons as discussed above, the condition for energy equilibrium for the large particles does not change from Eq. (40). For the small particles, the second-order moment equation contains two collisional contributions such that

$$\left(\frac{\partial P_{ij}}{\partial t}\right)_c = \int (v_i - u_i)(v_j - u_j)[C(f,f) + C(f,F)]d^3v \tag{131}$$

where

$$\int (v_i - u_i)(v_j - u_j) C(f,F) d^3v \equiv I \tag{132}$$

$$I = (R_{p,1} + R_{p,2})^2 \iiint (v_{1i}^* v_{1j}^* - v_{1i} v_{1j}) f(v_1) F(v_2) (\mathbf{g}\cdot\hat{\mathbf{k}})\, d\hat{\mathbf{k}}\, d^3 v_1\, d^3 v_2$$

and

$$\mathbf{v}_1^* = \mathbf{v}_1 - \frac{(1+\epsilon)m_2}{m_1 + m_2}(\mathbf{g}\cdot\hat{\mathbf{k}})\hat{\mathbf{k}} \quad . \tag{133}$$

If the dispersion-velocity distributions are analogous to that expressed in Eq. (24), the integral I may be transformed into a 6-dimensional integral as follows:

$$I = \frac{\pi(R_{p,1}+R_{p,2})^2 N_1 N_2}{4(2\pi)^3\sqrt{\det \mathbf{Q}}} \int \frac{(1+\epsilon)m_2}{m_1+m_2}\left[\frac{(1+\epsilon)m_2}{m_1+m_2}\right. \tag{134}$$

$$\times\left(\frac{g^2}{3}\delta_{ij}+g_i g_j\right)-(g_i h_j+h_i g_j)-2g_i g_j\Big]$$

$$\times g\exp\left(-\tfrac{1}{2}\mathbf{q}^T\cdot\mathbf{Q}^{-1}\cdot\mathbf{q}\right)d^6q$$

where

$$\mathbf{Q}=\begin{pmatrix}\mathbf{t}+\mathbf{T} & \mathbf{t}-\mathbf{T}\\ \mathbf{t}-\mathbf{T} & \mathbf{t}+\mathbf{T}\end{pmatrix},\quad \mathbf{q}=(g_x,g_y,g_z,h_x,h_y,h_z), \tag{135}$$

$$\mathbf{t}=\mathbf{p}/N_1 \text{ and } \mathbf{T}=\mathbf{P}/N_2$$

where $\mathbf{g}=\mathbf{v}_1-\mathbf{v}_2$ and $\mathbf{h}=\mathbf{v}_1+\mathbf{v}_2$. The anisotropy of the velocity distribution prevents an exact evaluation of the above integral. However, if we adopt the same approximation techniques as in Sec. II.B.2, by replacing a factor of g under the integral with a constant value $g_0=(16/3)\,[\mathrm{Tr}\,(\mathbf{t}+\mathbf{T})/6\pi]^{\frac{1}{2}}$, the integral becomes

$$I=\frac{4}{3}\,(R_{p,1}+R_{p,2})^2 N_1 N_2\left[\frac{\pi}{6}\,\mathrm{Tr}\,(\mathbf{t}+\mathbf{T})\right]^{\frac{1}{2}}\frac{[1+\epsilon(g_0)]m_2}{m_1+m_2}$$

$$\times\left\{\frac{[1+\epsilon(g_0)]m_2}{m_1+m_2}\left[\frac{1}{3}\,\mathrm{Tr}(\mathbf{t}+\mathbf{T})\delta_{ij}+t_{ij}+T_{ij}\right]-4t_{ij}\right\}. \tag{136}$$

In the above integration, we also approximated $\epsilon(v_c)$ by $\epsilon(g_0)$. The value of g_0 is so chosen as to provide the exact integral for the isotropic limit. Applying the above result into the second-order moment equation for the small particles, we find that t_{ij} is closely coupled to T_{ij}. Note that the impact velocity between small and large particles may be generally different from that among the two populations themselves. Therefore ϵ may assume a different value for different types of collisions even if ϵ is independent of particle size.

The solutions of the above equations may be obtained numerically for a given $\epsilon-v_c$ law (Stewart 1984). Preliminary results for the *ad hoc* prescription $\alpha = d\log(v_c^2)/d\log(1-\epsilon^2)$ are illustrated in Fig. 10 for different values of c_1/c_2 and τ_2. These results are in general agreement with those obtained from the heuristic discussion in Sec. VI.B.I. This agreement provides an *a posteriori* justification for the adopted approximation.

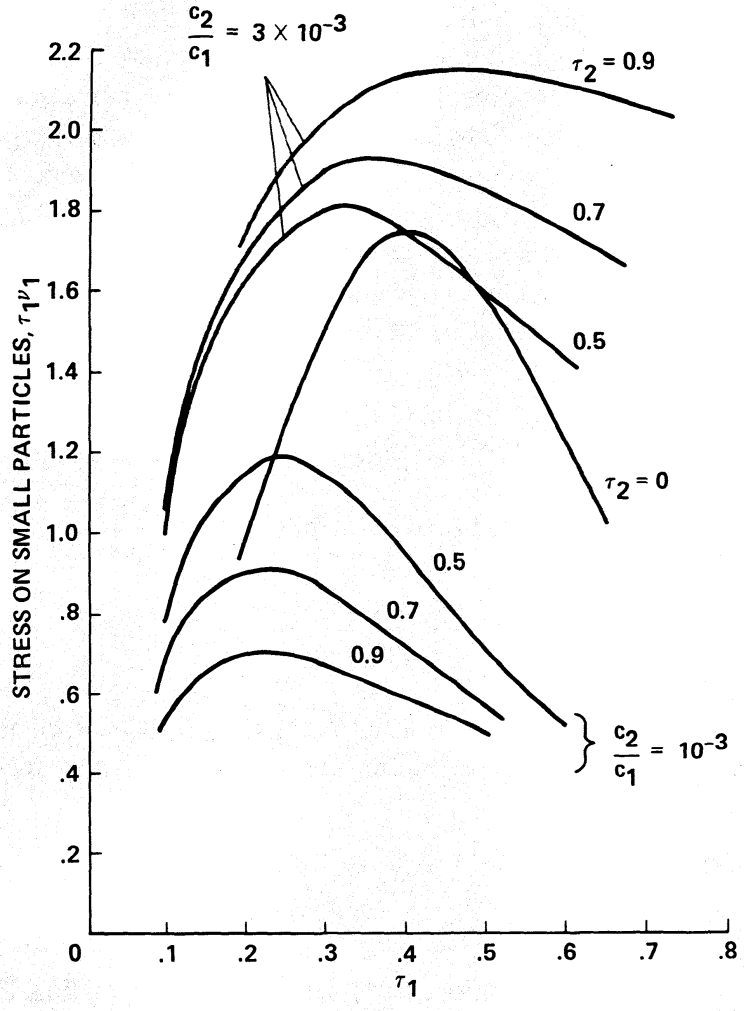

Fig. 10. Shear stress acting on small particles as a function of small particle optical depth τ, for various values of large particle optical depth τ_2 and two values of the velocity ratio c_2/c_1. For the smaller value of c_2/c_1, the finite value of c_2 has negligible effect. The velocity dependence of ϵ was assumed to be of the form $\alpha = d \log (v_c^2)/d \log (1 - \epsilon^2)$ with $\alpha = 10$.

C. Gravitational Effects on Small Particles

Rigorous analyses for gravitational scattering among ring particles would be considerably more complex than the above analyses for direct collisions. We mentioned some of the complications associated with gravitational scattering in Sec. V.A.1. A full-scale analysis would require a description modeled after Stewart and Kaula (1980) modified for the physical conditions appropriate to planetary rings. Nevertheless, a heuristic discussion, in the spirit of the preceding section, may be of interest (Cuzzi et al. 1979).

In a bimodal mass distribution where $m_1 << m_2$, the velocity deflection of a small particle passing a distance d from a much larger particle m_2 is of order $\Delta c_1 = 2Gm_2/(c_1 d)$. The corresponding change in the kinetic energy is $c_1 \Delta c_1$

$= 2Gm_2/d$. The frequency of such encounters is $\omega_{enc} = \pi d^2 N_2 c_1$ so that the rate of energy transfer between the two populations is $E_{grav} = 2\pi G m_2 N_2 c_1 d$. For a thin ring, most gravitational encounters occur over a distance $R_{p,2} < d < c_1/\Omega$. The cumulative effects of nearby and distant encounters may be approximated by the effect of one single encounter at a distance $d_{eff} = 2Gm_2/c_1^2$ so that $E_{grav} = 4\pi G^2 m_2^2 N_2/c_1$ (Cuzzi et al. 1979).

In addition to the energy change, gravitational scattering can also change the mean free path of the particles. To lowest order, the resultant change in the shear viscosity may be estimated in the same way as perfectly elastic collisions with collision frequency

$$\omega_{enc} \simeq 4\pi G^2 m_2^2 N_2 c_1^{-3} \approx \left[v_{esc}^4 c_1^{-3}/(c_2/\Omega + R_{p,2})\right]\tau_2 \ . \tag{137}$$

The straightforward extension of Eq. (118) is thus

$$\nu_1 = \frac{(\tau_1 + q\,\tau_2 + \omega_{enc}/\Omega)c_1^2}{\Omega\,[1 + (\tau_1 + q\,\tau_2 + \omega_{enc}/\Omega)^2]} \ . \tag{138}$$

If we insert this expression back into the energy equilibrium Eq. (55) and substitute ω_{enc} from Eq. (137) we obtain the following form of the energy equation:

$$\frac{(9/4)\,\Omega\,[\tau_1 + q\,\tau_2 + 4\pi G^2 m_2^2 N_2/(c_1^3\Omega)]\,c_1^2}{1 + [\tau_1 + q\,\tau_2 + 4\pi G^2 m_2^2 N_2/(c_1^3\Omega)]^2} = \omega_{1\to 1}(1-\epsilon^2)c_1^2 \ . \tag{139}$$

In the low-τ limit this expression agrees with the corresponding equation given by Cuzzi et al. (1979), who simply added $\dot{E}_{grav}$ to Eq. (55). In the limit of $\tau_1, \tau_2, \omega_{enc}/\Omega \gtrsim 1$, Eq. (139) must be used. This equation can be solved for the steady-state c_1; then the stress acting on the small particles is obtained from $\tau_1\nu_1$. This stress differs from that given by Ward and Harris (1983) who neglected to include the effect of ω_{enc} in the shear viscosity.

Gravitational scattering can also cause energy transfer from the large particles' random motion into the small particles' random internal motion. This dynamical friction effect was recently described in the context of the solar system accretion disk by Stewart and Kaula (1980). The resultant energy transfer rate will be negligible compared to the collisional energy transfer rate, Eq. (128), unless the velocity dispersion of the small particles falls below the escape velocity from the larger particles, $v_{esc} = (2Gm_2/R_{p,2})^{\frac{1}{2}}$. As in the case of direct collisions, the underlying energy source is derived from the systematic shearing motion. Therefore this source of energy must again be equivalent to an additional viscous stress. The above formula does not include this effect; the calculation could be done with the methods of Stewart and Kaula (1980).

In an energy equilibrium, a small optical depth corresponds to a large velocity dispersion so that gravitational scattering is relatively ineffective. For

a fixed ratio of τ_1/τ_2, the viscous stress due to gravitational scattering increases with τ since ω_{enc} increases with τ and c_1 decreases with τ. Therefore, gravitational scattering between the two populations again provides a stabilizing effect for the small particles. More detailed calculations are necessary to clairfy this effect, as it may depend sensitively on the validity of the 2-body scattering formula for ω_{enc}.

The above analysis for a bimodal distribution is a highly simplified attempt to account for a mass distribution of the form given by Eq. (114). Meaningful comparisons with observations may require a more general analysis where a realistic particle-size distribution is included.

VII. CONCLUSION

In this chapter, we have outlined the general formalism for calculating the structure, stability and viscous evolution of planetary rings. We have attempted to demonstrate the basic underlying physics with an idealized collision model for ring particles. For simplicity, much of the discussion is based on a uniform particle-size distribution and direct physical collisions. We also provided a limited discussion of additional effects due to nonuniform size distribution and gravitational interaction among the ring particles. The main conclusions that can be reached at the present time are as follows:

1. The steady-state structure of a particle disk is highly dependent on the degree of dissipation that occurs in collisions, i.e., the $\epsilon - v_c$ relation.
2. For the simple case of nongravitating hard spheres, thermal stability of a disk is assured provided that $d\epsilon^2/dE < 0$, where E is the energy of random motion. Thermal stability implies that the disk can reach an energy equilibrium at a finite scale height.
3. Equation (88) gives the conditions under which a viscous diffusion instability occurs, which may cause a ring system to break into many small ringlets separated by gaps with moderate optical depth. The occurrence of instability depends on the relationships between ϵ and v_c and between ϵ and τ. Preliminary experimental results for the $\epsilon - v_c$ relation for ice particles indicate that this mechanism could operate in Saturn's B Ring.
4. In regions of planetary rings with high optical depth, both the finite size of the particles as well as their mutual gravitational interaction produce important deviations from the hard-sphere model. These effects tend to enhance thermal stability and therefore to modify the requirement $d\epsilon^2/dE<0$. The criterion for diffusion instability is also modified to enhance stability at high τ.
5. A distribution of particle sizes can lead to more complicated size-selective diffusive instabilities. Preliminary analysis of a simple model with two particle sizes suggests that the diffusion instability for the smaller particles may occur at a smaller optical depth than for the larger

particles. This effect arises from the strong influence of the large particles on the dynamics of the small particles as opposed to the nearly negligible response of large particles to impacts of small particles. The resulting size segregation could lead to observable radial structure in the rings.

We can identify two directions for future investigations. First, it is important to analyze carefully and verify the several assumptions required for the kinetic theory of hard-sphere particle disks described in Sec. II. The traditional Boltzmann-equation formalism employed by Goldreich and Tremaine (1978) is based upon the approximate representation of Keplerian orbits as a random velocity dispersion about coplanar, circular orbits; the detailed dynamics of individual orbit changes as well as the systematic nature of the epicyclic motion is neglected in favor of collective conservation laws for total angular momentum and energy.

A more rigorous approach should formulate a Boltzmann equation directly in terms of the orbital elements of the particles (Hämeen-Anttila 1978). Since a particle's semimajor axis as well as the eccentricity and inclination is changed by a typical collision, the zeroth-order moment of Hämeen-Anttila's kinetic equation already describes the radial spreading of a particle disk. This treatment contrasts with the more traditional approach (described in Sec. II) in which the continuity equation must be supplemented by the first and second velocity moment equations so that a closed equation for the surface density evolution can be obtained. Nevertheless, by use of a Taylor expansion about the collisional change in semimajor axis and several additional approximations, Hämeen-Anttila obtains a coefficient of shear viscosity identical to our Eq. (53). More work is needed to relax some of the assumptions of previous work and to rederive our basic results in a more fundamental way. Such work should also lead to generalizations of the present results to more complicated situations, such as steep density gradients, where the hydrodynamic approximation breaks down.

Once the physics of the hard-sphere collision model in particle disks has been satisfactorily established, further investigation of more realistic collision models should be pursued in parallel with laboratory experiments on the collisional properties of candidate ring particle materials. Some of the complications which can arise in the event of particle aggregation and fragmentation, for example, are indicated by recent work on the protoplanetary disks of planetesimals (see chapters by Ward and by Weidenschilling et al.).

Future observations and further data analysis of the Voyager observations are needed to better constrain the size distribution of particles in Saturn's rings and the degree of size segregation associated with observed structure in the rings. Many component kinetic theories should help to elucidate these phenomena. The most complex structure appears in the denser portions of Saturn's B Ring where the effects of finite particle size and self-gravitation are expected to be important. A complete incorporation of these effects into the

kinetic theory will undoubtedly lead to complicated many-body effects. The wealth of phenomena known to occur in the theory of liquids compared to that of the ideal gas suggests many possible transport processes yet to be discovered in Saturn's rings.

Acknowledgments. This work was supported in part by National Science Foundation grants to the University of California at Santa Cruz. GRS was a NAS/NRC Resident Research Associate at NASA-Ames Research Center. The authors wish to thank J. Lissauer and J. Cuzzi for useful comments.

REFERENCES

Alfvén, H., and Arrhenius G. 1976. *Origin and Evolution of the Solar System*. (Washington, D.C.: NASA SP-345).

Anders, E. 1965. Fragmentation history of asteroids. *Icarus* 4:399–408.

Baxter, D. C., and Thompson, W. B. 1973. Elastic and inelastic scattering in orbital clustering. *Astrophys. J.* 183:323–336.

Boyd, T. J. M., and Sanderson, J. J. 1969. *Plasma Dynamics* (New York: Barnes and Noble), p. 51.

Brahic, A. 1977. Systems of colliding bodies in a gravitational field: I. Numerical simulation of the standard model. *Astron. Astrophys.* 54:895–907.

Brahic, A., and Hénon, M. 1977. Systems of colliding bodies in a gravitational field: II. Effect of transversal viscosity. *Astron. Astrophys.* 59:1–7.

Bridges, F. G., Hatzes, A., and Lin, D. N. C. 1984. On the structure, stability and evolution of Saturn's rings: Preliminary measurements of the coefficient of restitution of ice-ball collisions (preprint).

Cook, A. F., and Franklin, F. A. 1964. Rediscussion of Maxwell's Adams prize essay on the stability of Saturn's rings. *Astron. J.* 69:173–200.

Cuzzi, J. N., Durisen, R. H., Burns, J. A., and Hamill, P. 1979. The vertical structure and thickness of Saturn's rings. *Icarus* 38:54–68.

Faulkner, J., Lin, D. N. C., and Papaloizou, J. 1983. On the evolution of accretion disc flow in cataclysmic variables. I. The prospect of a limit cycle in dwarf nova systems. *Mon. Not. Roy. Astron. Soc.* 205:359–375.

Goldreich, P., and Tremaine, S. 1978. The velocity dispersion in Saturn's rings. *Icarus* 34:227–239.

Goldreich, P., and Tremaine, S. 1982. The dynamics of planetary rings. *Ann. Rev. Astron. Astrophys.* 20:249–284.

Goldsmith, W. 1960. *Impact* (London: Arnold).

Hämeen-Anttila, K. A. 1978. An improved and generalized theory for the collisional evolution of Keplerian systems. *Astrophys. Space Sci.* 58:477–519.

Hämeen-Anttila, K. A. 1981. Quasi-equilibrium in collisional systems. *Moon Planets* 25:477–506.

Hämeen-Anttila, K. A. 1982. Saturn's rings and bimodality of Keplerian systems. *Moon Planets* 26:171–196.

Hämeen-Anttila, K. A., and Lukkari, J. 1980. Numerical simulations of collisions in Keplerian systems. *Astrophys. Space Sci.* 71:475–497.

Harris, W. R., and Ward, A. W. 1983. On the radial structure of planetary rings. Proceedings of *I.A.U. Colloquium 75 Planetary Rings*, ed. A. Brahic, Toulouse, France, Aug. 1982.

Jeffreys, H. 1916. On certain possible distributions of meteoric bodies in the solar system. *Mon. Not. Roy. Astron. Soc.* 77:84–112.

Jeffreys, H. 1947. The effects of collisions on Saturn's rings. *Mon. Not. Roy. Astron. Soc.* 107:263–267.

Lane, A. L., Hord, C. W., West, R. A., Esposito, L. W., Coffeen, D. L., Sato, M., Simmons, K. E., Pomphrey, R. B., and Morris, R. B. 1982. Photopolarimetry from Voyager 2: Preliminary results on Saturn, Titan, and the rings. *Science* 215:537–543.

Lightman, A. P., and Eardley, D. M. 1974. Black holes in binary systems: Instability of disk accretion. *Astrophys. J.* 187:L1–L3.

Lin, D. N. C., and Bodenheimer, P. 1981. On the stability of Saturn's rings. *Astrophys. J.* 248:L83–L86.

Lin, D. N. C., and Bodenheimer, P. 1982. On the evolution of convective accretion disk models of the primitive solar nebula. *Astrophys. J.* 262:768–779.

Lissauer, J. J., Shu, F. H., and Cuzzi, J. N. 1983. Viscosity in Saturn's rings. Proceedings of *I.A.U. Colloquium 75 Planetary Rings*, ed. A. Brahic, Toulouse, France, Aug. 1982.

Lukkari, J. 1981. Collisional amplification of density fluctations in Saturn's rings. *Nature* 292:433–435.

Lynden-Bell, D., and Pringle, J. E. 1974. The evolution of viscous discs and the origin of the nebular variables. *Mon. Not. Roy. Astron. Soc.* 168:603–637.

Marouf, E. A., Tyler, G. L., Zebker, H. A., Simpson, R. A., and Eshleman, V. R. 1983. Particle size distributions in Saturn's rings from Voyager 1 radio occultation. *Icarus* 54:189–211.

Maxwell, J. C. 1859. On the stability of the motions of Saturn's rings. (Macmillan and Company, Cambridge and London). Also printed in *Scientific Papers of James Clerk Maxwell*. (Cambridge: Cambridge University Press, 1890), vol. 1.

Pringle, J. E., Rees, M. J., and Pacholczyk, A. G. 1973. Accretion onto massive black holes. *Astron. Astrophys.* 29:179–184.

Richtmyer, R. D. 1957. *Difference Methods for Initial Value Problems*. (New York: Interscience), ch. 6.

Safronov, V. S. 1969. Evolution of the protoplanetary cloud and formation of the Earth and planets. Nauka, Moscow, USSR, Transl. Israel Program for Sci. Transl., 1972, NASA TTF-677.

Salo, H., and Lukkari, J. 1982. Self-gravitation in Saturn's rings. *Moon Planets* 27:5–12.

Shakura, N. I., and Sunyaev, R. A. 1976. A theory of the instability of disk accretion onto black holes and the variability of binary X-ray sources, galactic nuclei and quasars. *Mon. Not. Roy. Astron. Soc.* 175:613–632.

Smith, B. A., Soderblom, L., Batson, R., Bridges, P., Inge, J., Masursky, H., Shoemaker, E., Beebe, R., Boyce, J., Briggs, G., Bunker, A., Collins, S. A., Hansen, C. J., Johnson, T. V., Mitchell, J. L., Terrile, R. J., Cook, A. F. II, Cuzzi, J., Pollack, J. B., Danielson, G. E., Morrison, D., Owen, T., Sagan, C., Veverka, J., Strom, R., and Suomi, V. 1982. A new look at the Saturn system: The Voyager 2 images. *Science* 215: 504–537.

Spitzer, L., Jr. 1962. *Physics of Fully Ionized Gases* (New York: Interscience).

Stewart, G. R. 1984. Dynamical effects of nonuniform particle size in Saturn's rings. Submitted to *Icarus*.

Stewart, G. R., and Kaula, W. M. 1980. A gravitational kinetic theory for planetesimals. *Icarus* 44:154–171.

Toomre, A. 1964. On the gravitational stability of a disk of stars. *Astrophys. J.*, 139:1217–1238.

Trulsen, J. 1971. Towards a theory of jet streams. *Astrophys. Space Sci.*, 12: 329–348.

Trulsen, J. 1972*a*. Numerical simulation of jet streams. I: The three-dimensional case. *Astrophys. Space Sci.* 17:241–262.

Trulsen, J. 1972*b*. Numerical simulation of jet streams. II: The two-dimensional case. *Astrophys. Space Sci.* 18:3–20.

Ward, W. R. 1981. On the radial structure of Saturn's rings. *Geophys. Res. Letters* 8:641–643.

Ward, W. R., and Harris, A. W. 1983. Diffusion instability in a bi-modal disc. In *Proceedings of IAU Colloquium 75, Planetary Rings*, ed. A. Brahic, Toulouse, France, Aug. 1982.